

Entanglement asymmetry in conformal field theory and holography

Francesco Benini^{a,b,c}, Victor Godet^{a,b}, Amartya Harsh Singh^{a,b}

^a *SISSA, Via Bonomea 265, 34136 Trieste, Italy*

^b *INFN, Sezione di Trieste, Via Valerio 2, 34127 Trieste, Italy*

^c *ICTP, Strada Costiera 11, 34151 Trieste, Italy*

Abstract

Entanglement asymmetry is a measure of symmetry breaking in quantum subsystems, inspired by quantum information theory, particularly suited to study out-of-equilibrium states. We study the entanglement asymmetry of a class of excited “coherent states” in conformal quantum field theories with a $U(1)$ symmetry, employing Euclidean path-integral methods with topological symmetry defects and the replica formalism. We compute, at leading order in perturbation theory, the asymmetry for a variety of subsystems, including finite spherical subregions in flat space, in finite volume, and at positive temperature. We also study its Lorentzian time evolution, showcasing the dynamical restoration of the symmetry due to thermalization, as well as the presence of a quantum Mpemba effect. Our results are universal, and apply in any number of dimensions. We also show that the perturbative entanglement asymmetry is related to the Fisher information metric, which has a known holographic dual called Hollands–Wald canonical energy, and that it is captured by the AdS bulk charge contained in the entanglement wedge.

Contents

1	Introduction	1
2	Entanglement asymmetry	3
3	Asymmetry for CFTs in the Rindler geometry	7
3.1	2d CFTs and replicas	8
3.2	Asymmetry as relative entropy	10
4	Other geometries, relaxation, and the Mpemba effect	12
4.1	Asymmetry for a finite subregion	14
4.2	Asymmetry at finite temperature and in finite volume	16
4.3	Time dependence and relaxation	17
4.4	Mpemba effect	20
5	Asymmetry in holography	24
5.1	Holographic setup	24
5.2	Asymmetry as canonical energy	27
5.3	Relation to the bulk charge	28
A	Renyi asymmetries in 2d CFTs	30
B	Computation from relative entropy	32
C	Asymmetry from twist operators	34
D	Embedding formalism	38

1 Introduction

Symmetry and symmetry breaking are key concepts in quantum field theory (QFT). Indeed, often it is only through the lenses of symmetry breaking that we decode the complicated dynamics of many-body systems or strongly-coupled QFTs. The traditional language to describe symmetry breaking is the Landau paradigm, *i.e.*, the analysis of the expectation values of local order parameters. On the other hand, quantum information theory has been playing over the years an increasingly important role in many-body systems and quantum field theory. For instance, in the context of QFT, quantum information can be used to derive monotonicity and positivity results [1–3]. In the context of AdS/CFT, quantum information allows us to understand the emergence of the bulk from the CFT [4, 5], to obtain the Page curve for toy models of evaporating black holes [6, 7], and it appears to be well-suited to study dynamics far from equilibrium [8].

Recently a new quantum information observable — dubbed *entanglement asymmetry* — has been introduced in [9] to detect and quantify symmetry breaking in quantum subsystems, in particular out of equilibrium. It is a modification of entanglement entropy. Given a reduced density matrix ρ that describes a pure or mixed state as seen from within a subsystem A , and given a $U(1)$ action on the Hilbert space, [9] proposes to compare ρ with the average of ρ over the adjoint action of $U(1)$, that we call ρ_Q .¹ Precisely, the entanglement asymmetry ΔS is defined as the difference between the entanglement entropies of ρ and ρ_Q , and it turns out to be equivalent to a relative entropy:

$$\Delta S = \text{Tr}(\rho \log \rho) - \text{Tr}(\rho_Q \log \rho_Q) = S(\rho \parallel \rho_Q). \quad (1.1)$$

This is a good measure of symmetry breaking: by known properties of relative entropy, ΔS is non-negative, and it vanishes if and only if the symmetry is unbroken in A .

Entanglement asymmetry was used in [9] to investigate a quantum version of the Mpemba effect [10–12] in spin chains. This is the phenomenon that excited symmetry-breaking states can relax and restore the symmetry faster than states in which the symmetry is less broken.² Such a counter-intuitive behavior is only possible far from equilibrium. Subsequent works that studied entanglement asymmetry and the Mpemba effect include [14–29].

In this paper we are interested in computing entanglement asymmetry in conformal quantum field theories (CFTs) with a $U(1)$ symmetry in general dimensions d , with an eye towards holography. In QFT, entanglement entropy is known to suffer from UV divergences. For entanglement asymmetry instead, being a relative entropy, the divergences cancel out and we expect to obtain a well-defined observable. In CFTs the vacuum does not spontaneously break the symmetry, thus we ought to consider some excited state. Here we study a class of “coherent states”, partially motivated by holography [30–32]:

$$|\Psi\rangle = e^{i\lambda V}|0\rangle, \quad (1.2)$$

obtained by acting on the vacuum with $e^{i\lambda V}$ in Euclidean time, where V is a primary local operator of charge 1.³ We choose to work in a perturbative expansion in λ , and show that $\Delta S = \lambda^2 \Delta S^{(2)} + O(\lambda^4)$. We compute the leading contribution $\Delta S^{(2)}$ in three different ways:

1. By first computing the Renyi asymmetries

$$\Delta S_n = \frac{1}{1-n} \left(\log \text{Tr} \rho_Q^n - \log \text{Tr} \rho^n \right) \quad (1.3)$$

using the replica method of [33–35], and then taking the limit $n \rightarrow 1$.

¹In fact this works for any group G : discrete, Abelian, and non-Abelian.

²Aristotle observed, some 2,300 years ago, that “to cool hot water quickly, begin by putting it in the sun”. The quantum Mpemba effect has been observed experimentally in ion traps [13].

³Similar states have been studied in [21].

2. By exploiting an integral representation for the leading perturbative contribution to relative entropy, also called Fisher information [32, 36].
3. By computing the Renyi asymmetries in terms of correlation functions of V and V^\dagger that include twist operators [34].

The result is a “universal expression” for the entanglement asymmetry, that depends on the dimension Δ of V and on the location of its insertion in Euclidean space.

It turns out that both $\Delta S^{(2)}$ and $\Delta S_n^{(2)}$ behave as two-point functions. This allows us (for instance as in [37]) to exploit conformal transformations to determine the entanglement asymmetry in a variety of geometries, for different choices of the subsystem A : for the “Rindler” geometry in which A is an infinite half-space; for finite spherical subregions A in infinite volume as well as in finite volume on S^{d-1} ; for spherical subregions on the hyperbolic plane \mathbb{H}^{d-1} at finite temperature; for finite intervals on the real line at finite temperature in $d = 2$.

Following [37, 38], we are also able to use conformal transformations and analytic continuation to determine the time evolution of entanglement asymmetry, starting from a coherent state (that we regard as originating from a local quench). As expected from thermalization, the asymmetry of a subsystem decreases with time since the excited state relaxes. Interestingly, however, we observe that a universal quantum Mpemba effect takes place.

In the context of AdS/CFT, what is the holographic dual to entanglement asymmetry? At leading order in λ , entanglement asymmetry is Fisher information, and the latter has a known holographic dual [36] given by a suitable integral of the so-called symplectic flux in the entanglement wedge. We observe that such a quantity can be recast in a suggestive form:

$$\Delta S^{(2)} = 2\pi \partial_{\tau_0} \left(\int_{\tilde{A}} \star F - \int_A \star F \right). \quad (1.4)$$

Here F is the field strength of the bulk gauge field dual to the $U(1)$ symmetry of the CFT, A is the chosen spatial subsystem at the boundary, \tilde{A} is the Ryu–Takayanagi surface (homologous to A) that describes entanglement entropy, while τ_0 is the boundary location of the insertion of V along the modular flow. This formula thus contains all the ingredients that we expect to be important in the holographic evaluation of entanglement asymmetry. We hope to be able to address the higher-order terms, and to obtain a better physical understanding of this formula, in future work.

2 Entanglement asymmetry

Let us review the definition of entanglement asymmetry proposed in [9].⁴ Consider a quantum system which can be divided into two parts A and B in such a way that the Hilbert space

⁴The authors of [39] considered a very similar quantity, but for global states.

factorizes: $\mathcal{H} = \mathcal{H}_A \otimes \mathcal{H}_B$. Given a (normalized) density matrix ρ_{tot} , which could represent a pure ($\rho_{\text{tot}} = |\psi\rangle\langle\psi|$) or a mixed state, one constructs the reduced density matrix on A , namely $\rho = \text{Tr}_B \rho_{\text{tot}}$, and its entanglement entropy is given by the von Neumann entropy $S = -\text{Tr}(\rho \log \rho)$. Consider the case that there exists a charge operator Q that generates a $U(1)$ action on the Hilbert space,⁵ and that the charge operator can be factorized as well:

$$Q = Q_A \otimes \mathbb{1}_B + \mathbb{1}_A \otimes Q_B. \quad (2.1)$$

If the state ρ_{tot} is an eigenstate of Q , namely $[\rho_{\text{tot}}, Q] = 0$ and thus the symmetry is unbroken, then $[\rho, Q_A] = 0$ and thus ρ takes a block-diagonal form in a basis of eigenspaces of Q_A . Then the entanglement entropy S can be resolved into the contributions $S(q)$ from each charge sector: this is called symmetry-resolved entanglement entropy [40–42]. On the other hand, if the symmetry is broken in the subsystem A and thus $[\rho, Q_A] \neq 0$, one can quantify the amount of breaking in the following way. One constructs a projected reduced density matrix

$$\rho_Q = \sum_{q \in \mathbb{Z}} \Pi_q \rho \Pi_q, \quad (2.2)$$

where Π_q is the projector to the eigenspace of Q_A with charge q . This is essentially the matrix ρ with all off-diagonal blocks set to zero. The quantity (2.2) can be recast in a more elegant form by using the Fourier transform of the projector $\Pi_q = \int_0^{2\pi} \frac{d\alpha}{2\pi} e^{i\alpha(Q_A - q)}$, hence

$$\rho_Q = \int_0^{2\pi} \frac{d\alpha}{2\pi} e^{-i\alpha Q_A} \rho e^{i\alpha Q_A}. \quad (2.3)$$

This is the average of ρ over the adjoint action of the group $U(1)$, and it naturally generalizes to discrete as well as non-Abelian groups [16–18, 23]. Notice that ρ_Q is a density matrix, namely it is Hermitian, semi-positive definite, and $\text{Tr} \rho_Q = 1$. The entanglement asymmetry is defined as the difference between the entanglement entropies of ρ_Q and ρ [9]:

$$\Delta S = S[\rho_Q] - S[\rho] = \text{Tr}(\rho \log \rho) - \text{Tr}(\rho_Q \log \rho_Q). \quad (2.4)$$

One easily verifies that the entanglement asymmetry is equivalent to the relative entropy of ρ with respect to ρ_Q [39]:

$$\Delta S = \text{Tr}(\rho (\log \rho - \log \rho_Q)) = S(\rho \parallel \rho_Q). \quad (2.5)$$

This makes ΔS a good measure of symmetry breaking. Indeed, as it follows from the properties of relative entropy: $\Delta S \geq 0$, and $\Delta S = 0$ if and only if $\rho = \rho_Q$ namely if $[\rho, Q_A] = 0$ so that the symmetry is unbroken in A .

⁵In most cases, and in this paper too, the $U(1)$ action is a global symmetry of the quantum system. However the Hamiltonian of the system does not enter into the definition of entanglement asymmetry and therefore one could consider $U(1)$ actions that are not symmetries, as for instance in [23].

The entanglement asymmetry can be obtained from Renyi entanglement asymmetries using the replica trick [33, 34]. The Renyi entanglement asymmetries are defined as

$$\Delta S_n = \frac{1}{1-n} \log \frac{\text{Tr}(\rho_Q^n)}{\text{Tr}(\rho^n)}. \quad (2.6)$$

The entanglement asymmetry is obtained from the limit $\Delta S = \lim_{n \rightarrow 1} \Delta S_n$. The moments $\text{Tr}(\rho_Q^n)$ are easily obtained from (2.3). By a change of integration variables, they can be written as [9, 39]:

$$\text{Tr}(\rho_Q^n) = \int_0^{2\pi} \frac{d\gamma_1 \dots d\gamma_{n-1}}{(2\pi)^{n-1}} X_n(A, \gamma) \quad (2.7)$$

where we defined the so-called charged moments

$$X_n(A, \gamma) = \text{Tr} \left[\rho e^{i\gamma_1 Q_A} \rho e^{i\gamma_2 Q_A} \dots \rho e^{i\gamma_{n-1} Q_A} \rho e^{-i(\gamma_1 + \dots + \gamma_{n-1}) Q_A} \right]. \quad (2.8)$$

We could formally define $\gamma_n \equiv -(\gamma_1 + \dots + \gamma_{n-1})$ so that $\sum_{j=1}^n \gamma_j = 0$. Thus, the charged moments implement all insertions of elements of $U(1)$ that multiply to the identity.

We are interested in studying entanglement asymmetry in quantum field theories, following [34]. In particular, we will use the path integral over replicas in order to define and compute traces of density matrices. It is well known that the definition of entanglement entropy we presented is plagued by UV divergences when used in quantum field theory, as opposed to quantum mechanics. The situation improves for entanglement asymmetry (as it does in general for relative entropies) because the divergences cancel among the numerator and denominator of (2.6), at least as long as the symmetry breaking is spontaneous, or explicit but soft.

We consider states ρ_{tot} that have a Euclidean path-integral representation. In particular, given a spatial manifold \mathcal{M} , the state ρ_{tot} is produced by the path integral on some Euclidean manifold, possibly with operator insertions, with a cut along a copy of \mathcal{M} . We call this geometry \mathcal{G} . Schematically, the matrix elements of such a state are

$$\langle \phi_- | \rho_{\text{tot}} | \phi_+ \rangle = \frac{1}{Z} \int_{\substack{\text{geometry } \mathcal{G} \\ \varphi(0^-, \mathcal{M}) = \phi_- \\ \varphi(0^+, \mathcal{M}) = \phi_+}} \mathcal{D}\varphi(\dots) e^{-S[\varphi]}. \quad (2.9)$$

Here (t_E, \mathcal{M}) are Euclidean coordinates with t_E the Euclidean time and the cut at $t_E = 0$, ϕ_{\mp} are Dirichlet boundary conditions for the fields, (\dots) are possible operator insertions, while Z is the partition function on \mathcal{G} with the cut closed so as to guarantee that $\text{Tr} \rho_{\text{tot}} = 1$. The reduced density matrix ρ is obtained by partially closing the cut along B while keeping it open along $A \subset \mathcal{M}$. The moments of ρ are computed by

$$\text{Tr}(\rho^n) = \frac{Z_n(A)}{Z^n}. \quad (2.10)$$

Here $Z_n(A)$ is the Euclidean path integral of the theory on a manifold \mathcal{G}_n obtained by gluing together n identical copies of \mathcal{G} (possibly with operator insertions) along the cut A , in such a

way that the lower part of the cut on the n -th copy is glued to the upper part of the cut on the $(n + 1)$ -th copy. Then $Z \equiv Z_1(A)$ is the path integral on \mathcal{G} (possibly with operator insertions) with the cut completely closed.

In order to compute the charged moments $X_n(A, \gamma)$ of ρ_Q we need to insert the operators $e^{i\gamma_j Q_A}$ into the trace [23]. In the path-integral description they are the topological codimension-one surfaces $U_\gamma[A]$, also called symmetry defects, that implement the $U(1)$ action on the Hilbert space [43], placed along the cut A . They are

$$U_\gamma[A] = \exp\left(i\gamma \int_A \star J\right) \quad \text{labelled by } \gamma \in [0, 2\pi) \cong U(1), \quad (2.11)$$

where J is the conserved $U(1)$ current operator, while \star is the Hodge star operation. Thus

$$X_n(A, \gamma) = \frac{Z_n(A, \gamma)}{Z^n}. \quad (2.12)$$

Here $Z_n(A, \gamma)$ is the path integral on \mathcal{G}_n with the insertion of topological symmetry defects $U_{\gamma_j}[A]$ along each of the gluings from one replica to the next. In the original geometry \mathcal{G} it may appear that the operator $U_\alpha[A]$ has a boundary along ∂A , and in general the boundaries of symmetry defect operators are *not* topological. However on the covering geometry \mathcal{G}_n there are n symmetry defects that join along ∂A and with parameters γ_j that sum up to $0 \in U(1)$, therefore in this case the junction of defects is topological as well.⁶ Notice that $Z_1(A, \gamma) = Z$.

Eventually, the path-integral formula for the Renyi asymmetries is

$$\Delta S_n = \frac{1}{1-n} \log \frac{\frac{1}{(2\pi)^{n-1}} \int d\vec{\gamma} Z_n(A, \gamma)}{Z^n(A)}, \quad (2.13)$$

where $d\vec{\gamma}$ is a shorthand notation for $d\gamma_1 \dots d\gamma_{n-1}$. Similar partition functions with topological defects were recently considered in [44] to study entanglement entropy in symmetric product orbifold CFTs.

There exists an alternative computational approach in which one considers n replicas of the theory, as opposed to n replicas of the Euclidean geometry. In this approach one computes the path integral of the theory in the presence of twist fields placed along ∂A that implement the gluing of one copy of the theory to the next as one crosses A [34]. In the context of entanglement asymmetry, the twist fields are dressed by the endpoints of a suitable symmetry defect placed along A [17, 23]. We illustrate and utilize this approach in Appendix C.

⁶In the presence of an 't Hooft anomaly for the $U(1)$ symmetry, one may be worried that the path-integral definition of Renyi asymmetries is plagued by phase ambiguities: indeed one needs to resolve the junction of n symmetry defects into a network of trivalent junctions, and different choices are related by nontrivial phases in the presence of an 't Hooft anomaly (we thank Giovanni Galati for raising this issue). In two dimensions each connected component of A is an interval with two ends. We insist that the resolution of the junction be specular on the two ends: in this way, if one changes the resolution one obtains conjugate phases from the two ends and they cancel each other. In higher dimensions each connected component of A has a connected boundary, and we similarly insist that the resolution be “constant” along that boundary. We leave a more detailed study of possible effects of 't Hooft anomalies and higher-group structures on entanglement asymmetry for the future.

of length $^\Delta$ and thus we study a limit in which λ is small compared to the Euclidean distance between the insertion point z_- and the cut A . In the denominator of (3.2) we find

$$\langle \mathcal{O}_1 \mathcal{O}_1^\dagger \dots \mathcal{O}_n \mathcal{O}_n^\dagger \rangle_{\mathcal{G}_n} = 1 + \lambda^2 \sum_{j,k} \langle V(z_{j-}) V^\dagger(z_{k+}) \rangle_{\mathcal{G}_n} + O(\lambda^4). \quad (3.3)$$

Notice that there are no terms with odd powers of λ because of charge conservation in the vacuum. Besides, at order λ^2 we never pick up the product of two V 's or two V^\dagger 's at the same point and therefore we do not have to worry about divergences. In the numerator of (3.2) we have a correlator in the presence of the symmetry defects \mathcal{L}_{γ_j} . Since they are topological, we can swipe them through the replicas until they are all moved to the same sheet, and then we can collapse them on top of each other. Since the parameters sum up to zero, they disappear. However, when they cross a local operator, the correlator picks up a phase. We thus find

$$\langle \mathcal{O}_1 \mathcal{O}_1^\dagger \mathcal{L}_{\gamma_1} \dots \mathcal{O}_n \mathcal{O}_n^\dagger \mathcal{L}_{\gamma_n} \rangle_{\mathcal{G}_n} = 1 + \lambda^2 \sum_{j,k} e^{i\theta_{jk}} \langle V(z_{j-}) V^\dagger(z_{k+}) \rangle_{\mathcal{G}_n} + O(\lambda^4), \quad (3.4)$$

where $\theta_{jk} = \sum_{i=j}^{k-1} \gamma_i$ if $k > j$, or $\theta_{jk} = -\sum_{i=k}^{j-1} \gamma_i$ if $k < j$, or $\theta_{jk} = 0$ if $j = k$. Once we integrate in $d\vec{\gamma}$, all terms in the summation with a nontrivial phase are projected out, therefore the summation reduces to $j = k$:

$$\frac{1}{(2\pi)^{n-1}} \int d\vec{\gamma} \langle \mathcal{O}_1 \mathcal{O}_1^\dagger \mathcal{L}_{\gamma_1} \dots \mathcal{O}_n \mathcal{O}_n^\dagger \mathcal{L}_{\gamma_n} \rangle_{\mathcal{G}_n} = 1 + \lambda^2 \sum_j \langle V(z_{j-}) V^\dagger(z_{j+}) \rangle_{\mathcal{G}_n} + O(\lambda^4). \quad (3.5)$$

In other words, the integral projects to covering geometries in which the total charge vanishes copy by copy, not just globally in the union of copies. From (3.2) we eventually obtain

$$\Delta S_n = \frac{\lambda^2}{n-1} \sum_{j \neq k}^n \langle V(z_{j-}) V^\dagger(z_{k+}) \rangle_{\mathcal{G}_n} + O(\lambda^4). \quad (3.6)$$

This gives the leading perturbative contribution to the Renyi asymmetries.

3.1 2d CFTs and replicas

Two-point functions on the replicated geometries \mathcal{G}_n are non-trivial because the branching loci ∂A create curvature singularities. The two-dimensional case is special because, in certain cases, the singularities can be removed by a conformal transformation. We thus consider a 2d CFT, and the case that A is the semi-infinite line to the right of the origin. Using a complex coordinate $z = z_2 + iz_1$ (where z_1 is Euclidean time and z_2 is space) we take $A = \{z \in \mathbb{R}_+\}$. We call this case the *Rindler geometry*, as in Fig. 2 left (we will consider other geometries in Section 4). We can then compute correlators on \mathcal{G}_n by exploiting a conformal covering map $\zeta = z^{1/n}$. Two-point functions transform as

$$\langle V(z_{j-}) V^\dagger(z_{k+}) \rangle_{\mathcal{G}_n} = \left| \frac{d\zeta}{dz}(\zeta_{j-}) \frac{d\zeta}{dz}(\zeta_{k+}) \right|^\Delta \langle V(\zeta_{j-}) V^\dagger(\zeta_{k+}) \rangle_{\mathbb{C}}, \quad (3.7)$$

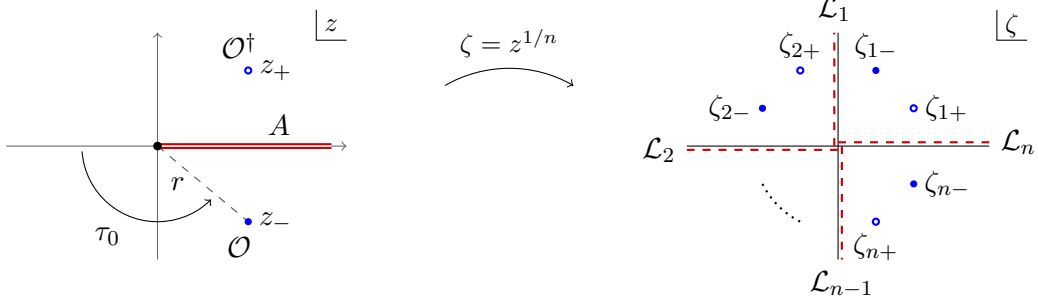


Figure 2: Left: physical z -plane of the Rindler geometry, with insertions of \mathcal{O} at $z_- = r e^{-i(\pi-\tau_0)}$ and \mathcal{O}^\dagger at $z_+ = z_-^*$. Right: covering ζ -plane, in the case $n = 4$. The conformal map is $\zeta = z^{1/n}$.

where Δ is the dimension of V . We parametrize the insertion points z_\pm as

$$z_- = r e^{-i(\pi-\tau_0)}, \quad z_+ = r e^{i(\pi-\tau_0)}, \quad r > 0, \quad 0 < \tau_0 < \pi. \quad (3.8)$$

On the covering ζ -plane we take

$$\zeta_{j-} = r^{1/n} e^{i[2\pi(j-\frac{1}{2})+\tau_0]/n}, \quad \zeta_{j+} = r^{1/n} e^{i[2\pi(j-\frac{1}{2})-\tau_0]/n}. \quad (3.9)$$

The twist lines \mathcal{L}_j (before being removed) run along the semi-infinite lines with $\arg(\zeta) = 2\pi j/n$, as depicted in Fig. 2 right. The two-point functions on the covering geometries \mathcal{G}_n are

$$\langle V(z_{j-}) V^\dagger(z_{k+}) \rangle_{\mathcal{G}_n} = \frac{1}{n^{2\Delta} r^{2\Delta(n-1)/n} |\zeta_{j-} - \zeta_{k+}|^{2\Delta}}. \quad (3.10)$$

Writing the Renyi asymmetry as $\Delta S_n = \lambda^2 \Delta S_n^{(2)} + O(\lambda^4)$, the leading term from (3.6) is

$$\Delta S_n^{(2)} = \frac{n^{-2\Delta}}{n-1} \frac{1}{r^{2\Delta}} \sum_{j \neq k}^n \frac{1}{|2 \sin(\frac{\tau_0 + (j-k)\pi}{n})|^{2\Delta}}. \quad (3.11)$$

In order to compute the leading contribution $\Delta S^{(2)}$ to the entanglement asymmetry we need to analytically continue (3.11) to complex values of n and then take the limit $n \rightarrow 1$. This means that we need to perform the sum explicitly. We were able to do that only for some integer values of 2Δ , using the Mellin transform

$$\frac{1}{\sin(\pi x)} = \frac{1}{\pi} \int_{\mathbb{R}} ds \frac{e^{sx}}{1+e^s} \quad \text{for } 0 < \text{Re}(x) < 1. \quad (3.12)$$

In Appendix A we perform the computation for $\Delta = \frac{1}{2}, 1, \frac{3}{2}, 2$. For instance, for $\Delta = 1$ the Renyi asymmetry of the Rindler geometry takes the form

$$\Delta = 1 : \quad \Delta S_n^{(2)} = \frac{1}{4r^2} \frac{n}{n-1} \left(\frac{1}{\sin^2(\tau_0)} - \frac{1}{n^2 \sin^2(\frac{\tau_0}{n})} \right), \quad (3.13)$$

therefore the entanglement asymmetry is

$$\Delta = 1 : \quad \Delta S_{\text{Rindler}}^{(2)} = \frac{1}{2r^2 \sin^2(\tau_0)} \left(1 - \frac{\tau_0}{\tan(\tau_0)} \right). \quad (3.14)$$

In the next section we will determine $\Delta S_{\text{Rindler}}^{(2)}$ for all $\Delta \in \mathbb{R}_+$.

3.2 Asymmetry as relative entropy

We can make progress in the computation of the leading contribution to the entanglement asymmetry of coherent states in a perturbative expansion in λ — in general dimension d — by using that entanglement asymmetry is a relative entropy.

Given two density matrices ρ_0, ρ_1 , their relative entropy is defined as

$$S(\rho_1 \parallel \rho_0) = \text{Tr}(\rho_1 \log \rho_1) - \text{Tr}(\rho_1 \log \rho_0). \quad (3.15)$$

Consider a continuous family $\rho(\lambda) = \rho_0 + \lambda \delta\rho + O(\lambda^2)$, normalized so that $\text{Tr} \rho(\lambda) = 1$. Then, the relative entropy $S(\rho(\lambda) \parallel \rho_0)$ starts at second order in λ and at that order it is given by

$$\frac{1}{2} \frac{d^2}{d\lambda^2} S(\rho(\lambda) \parallel \rho_0) = F(\delta\rho, \delta\rho)_{\rho_0}, \quad (3.16)$$

where the quantity $F(\delta\rho_1, \delta\rho_2)_{\rho_0}$ is symmetric in its arguments and is called the Fisher information metric around ρ_0 . There exists an integral formula for it, see *e.g.* Appendix B of [32]:

$$F(\delta\rho_1, \delta\rho_2)_{\rho_0} = \frac{1}{4} \int_{-\infty}^{\infty} \frac{ds}{1 + \cosh(s)} \text{Tr} \left[\delta\rho_1 \rho_0^{-\frac{1}{2} - \frac{is}{2\pi}} \delta\rho_2 \rho_0^{-\frac{1}{2} + \frac{is}{2\pi}} \right]. \quad (3.17)$$

This formula is valid even if $\rho(\lambda)$ is not Hermitian, as long as it is normalized.

In our setup the reduced density matrix ρ is

$$\rho = \sigma + \lambda \sigma (iV - iV^\dagger) + O(\lambda^2), \quad (3.18)$$

where $\sigma = \text{Tr}_B |0\rangle\langle 0|$ is the reduced density matrix of the vacuum. Since the vacuum does not break the symmetry while $\sum_q \Pi_q \sigma V \Pi_q = 0$, we obtain that the projection ρ_Q differs from the vacuum only at second order in λ : $\rho_Q = \sigma + O(\lambda^2)$. We already noticed that the entanglement asymmetry can be written as a relative entropy $\Delta S = S(\rho \parallel \rho_Q)$. Using again that σ commutes with Q_A , we can also write the asymmetry as $\Delta S = S(\rho \parallel \sigma) - S(\rho_Q \parallel \sigma)$. Since ρ_Q is equal to σ at first order in λ , the second term does not contribute at leading order. We thus obtain

$$\Delta S = \lambda^2 S^{(2)}(\rho \parallel \sigma) + O(\lambda^4). \quad (3.19)$$

We apply this formula to the Rindler geometry in $d \geq 2$ dimensions. The spatial slice is \mathbb{R}^{d-1} , the subsystem A is a half-space, and the entangling surface ∂A is a $(d-2)$ -dimensional plane. We use a complex coordinate z for the spatial direction orthogonal to the entangling surface and the Euclidean time direction, and y_i for the other coordinates (if any). The state is obtained from the vacuum with the insertion of $\mathcal{O} = e^{i\lambda V}$ at z_- and $\mathcal{O}^\dagger = e^{-i\lambda V^\dagger}$ at $z_+ = z_-^*$, both on the plane $y_i = 0$. We could more generally consider insertions at two generic points, not necessarily related by complex conjugation.⁸ We will be interested in the case

$$z_- = r e^{-i(\pi - \tau_-)} = r e^{i\theta_-}, \quad z_+ = r e^{i(\pi - \tau_+)} = r e^{i\theta_+}. \quad (3.20)$$

⁸In this case the Euclidean path integral prepares a non-Hermitian matrix.

The reduced density matrix σ of the vacuum in the Rindler geometry is special because its modular Hamiltonian K defined by $\sigma = e^{-K}$ is local and geometric: it generates a counter-clockwise rotation of the complex coordinate z around the entangling surface. We can thus write the state ρ as

$$\begin{aligned}\rho &= e^{-\left(1-\frac{\theta_-}{2\pi}\right)K} e^{i\lambda V} e^{-\frac{\theta_- - \theta_+}{2\pi}K} e^{-i\lambda V^\dagger} e^{-\frac{\theta_+}{2\pi}K} \\ &= \sigma + i\lambda \sigma e^{\frac{\theta_-}{2\pi}K} V e^{-\frac{\theta_-}{2\pi}K} - i\lambda \sigma e^{\frac{\theta_+}{2\pi}K} V^\dagger e^{-\frac{\theta_+}{2\pi}K} + O(\lambda^2) \\ &= \sigma + i\lambda \sigma V(z_-) - i\lambda \sigma V^\dagger(z_+) + O(\lambda^2),\end{aligned}\tag{3.21}$$

as already written in (3.18). To this state we apply (3.16)–(3.17). Taking into account charge conservation, we obtain two terms which however are equal using the change of variable $s \rightarrow -s$ and the cyclicity of the trace:

$$\Delta S_{\text{Rindler}}^{(2)} = \frac{1}{2} \int \frac{ds}{1 + \cosh(s)} \text{Tr} \left[\sigma V^\dagger(z_+) \sigma^{-\frac{1}{2} - \frac{is}{2\pi}} \sigma V(z_-) \sigma^{-\frac{1}{2} + \frac{is}{2\pi}} \right].\tag{3.22}$$

Shifting the integration contour as $s \rightarrow s + \pi i(1 - \varepsilon)$ where ε is an infinitesimal positive quantity that specifies a contour prescription, the integral is recast as

$$\Delta S_{\text{Rindler}}^{(2)} = -\frac{1}{4} \int \frac{ds}{\sinh^2\left(\frac{s}{2} - i\varepsilon\right)} \text{Tr} \left[\sigma \sigma^{-\frac{is}{2\pi}} V(z_-) \sigma^{\frac{is}{2\pi}} V^\dagger(z_+) \right].\tag{3.23}$$

The trace contains operators time-ordered with respect to modular time and is thus a two-point function. With $s = 0$, if we take two generic ordered points $z_j = e^{u_j + i\theta_j}$ we have

$$\begin{aligned}\text{Tr} \left[\sigma V(z_1) V^\dagger(z_2) \right] &= \langle V(z_1) V^\dagger(z_2) \rangle = \frac{1}{|z_1 - z_2|^{2\Delta}} = \\ &= \frac{1}{\left[2e^{u_1 + u_2} (\cosh(u_1 - u_2) - \cos(\theta_1 - \theta_2)) \right]^\Delta} \equiv G_\Delta(u_1, \theta_1, u_2, \theta_2).\end{aligned}\tag{3.24}$$

Since $V(z_-) = e^{\frac{\theta_-}{2\pi}K} V(r, 0) e^{-\frac{\theta_-}{2\pi}K}$ we see that $\sigma^{-\frac{is}{2\pi}} V(z_-) \sigma^{\frac{is}{2\pi}}$ has the net effect of shifting $\theta_- \rightarrow \theta_- + is$. The trace in (3.23) is then $G_\Delta(u, \theta_- + is, u, \theta_+) = G_\Delta(u, \pi + \tau_- + is, u, \pi - \tau_+)$ in terms of our parametrization. We obtain the formula:

$$\Delta S_{\text{Rindler}}^{(2)} = - \int_{-\infty}^{+\infty} \frac{ds}{4r^{2\Delta} \sinh^2\left(\frac{s}{2} - i\varepsilon\right) \left[-4 \sinh^2\left(\frac{s}{2} - i\tau_0\right) \right]^\Delta}\tag{3.25}$$

where $\tau_0 = \frac{1}{2}(\tau_+ + \tau_-)$.

As we describe in Appendix B, the integral in (3.25) can be analytically performed in terms of a hypergeometric function. Let us define the function:⁹

$$I_\Delta(x) = \frac{\sqrt{\pi} \Gamma(\Delta + 1)}{4^\Delta \Gamma(\Delta + \frac{1}{2})} \left(1 - (1 - x^2) \frac{\Delta}{\Delta + \frac{1}{2}} {}_2F_1 \left[1, \frac{1}{2} - \Delta, \frac{3}{2} + \Delta; -x^2 \right] \right).\tag{3.26}$$

⁹Recall that ${}_2F_1(a, b, c; z) = \sum_{n=0}^{\infty} \frac{(a)_n (b)_n}{(c)_n} \frac{z^n}{n!}$ and in particular ${}_2F_1(a, b, c; 0) = 1$. The analytic continuation for $|z| \geq 1$ has a branch cut from 1 to ∞ along the positive real axis.

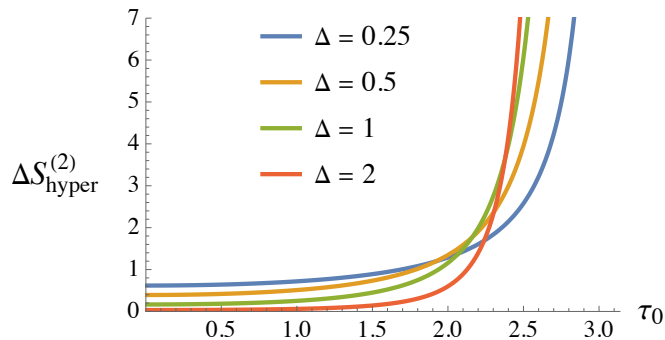


Figure 3: The function $I_{\Delta}(\tan(\frac{\tau_0}{2}))$ that describes $\Delta S_{\text{Rindler}}^{(2)}$ and $\Delta S_{\text{hyper}}^{(2)}$, plotted for different values of Δ as a function of $\tau_0 \in [0, \pi)$.

Then

$$\Delta S_{\text{Rindler}}^{(2)} = \frac{1}{r^{2\Delta}} I_{\Delta}\left(\tan\left(\frac{\tau_0}{2}\right)\right). \quad (3.27)$$

The entanglement asymmetry of the Rindler geometry starts at a finite value for $\tau_0 = 0$ and increases monotonically with a divergence at $\tau_0 = \pi$ with the following behaviors:¹⁰

$$\lim_{\tau_0 \rightarrow 0} \Delta S_{\text{Rindler}}^{(2)} = \frac{\sqrt{\pi} \Gamma(\Delta + 1)}{2(2r)^{2\Delta} \Gamma(\Delta + \frac{3}{2})}, \quad \Delta S_{\text{Rindler}}^{(2)} \underset{\tau_0 \rightarrow \pi}{\sim} \frac{2\pi\Delta}{(2r)^{2\Delta} \sin^{2\Delta+1}(\tau_0)}. \quad (3.28)$$

This is illustrated in Fig. 3 where we plot the function $I_{\Delta}(\tan(\tau_0/2))$ for different values of Δ . For semi-integer values of Δ we found alternative expressions for (3.25) in terms of trigonometric functions. For $\Delta \in \frac{1}{2} + \mathbb{Z}_{\geq 0}$ we found the expressions:

$$\Delta S_{\text{Rindler}}^{(2)} = \frac{\pi \Delta}{(4r)^{2\Delta} \cos^{2\Delta+1}(\frac{\tau_0}{2})} \left[1 + \sum_{k=1}^{\Delta-\frac{3}{2}} \frac{(\Delta - \frac{1}{2} - k) (\Delta - \frac{3}{2} + k)!}{k! (\Delta - \frac{1}{2})!} \cos^{2k}\left(\frac{\tau_0}{2}\right) \right]. \quad (3.29)$$

The summation is finite and contributes only for $\Delta \geq \frac{5}{2}$. For $\Delta \in \mathbb{Z}_{\geq 1}$ we found:

$$\Delta S_{\text{Rindler}}^{(2)} = \frac{2\Delta}{(2r)^{2\Delta} \sin^{2\Delta}(\tau_0)} \left[1 - \frac{\tau_0}{\tan(\tau_0)} - \sum_{k=1}^{\Delta-1} \frac{(2k-2)!!}{(2k+1)!!} \sin^{2k}(\tau_0) \right]. \quad (3.30)$$

The summation is finite and contributes only for $\Delta \geq 2$. These expressions match with those we already found in $d = 2$ for $\Delta = \frac{1}{2}, 1, \frac{3}{2}, 2$ using the replica method (see Appendix A).

4 Other geometries, relaxation, and the Mpemba effect

For the class of states (3.1) and at leading order in λ , it is clear from (3.6) that both Renyi and entanglement asymmetries behave as two-point functions. This means that in a CFT we can

¹⁰They follow from $\lim_{x \rightarrow 0} I_{\Delta}(x) = \frac{\sqrt{\pi} \Gamma(\Delta + 1)}{2^{2\Delta+1} \Gamma(\Delta + 3/2)}$ and $I_{\Delta}(x) \sim \frac{\pi \Delta}{16^{\Delta}} x^{2\Delta+1}$ for $x \rightarrow +\infty$.

exploit conformal transformations to determine the asymmetry in geometries other than the Rindler one.¹¹ In this section we will compute the entanglement asymmetry of finite spherical regions A in arbitrary dimensions, both in infinite volume, in a finite spherical volume, and in the hyperbolic plane at finite temperature.¹²

By analytic continuation from Euclidean to Lorentzian time, we will also be able to compute the time evolution of entanglement asymmetry in those geometries. Thus entanglement asymmetry can be used to study dynamics: starting with a state that explicitly breaks the symmetry (in our setup regarded as a local quench at $t = 0$) we can study the dynamical restoration of the symmetry as expected from thermalization. In the context of quantum spin chains, entanglement asymmetry was used in [9] and subsequent works to provide a quantitative framework to study the Mpemba effect [10–12] — the observation that states farther away from equilibrium can relax faster. We observe a similar effect for the coherent states in CFTs in general dimensions.

First of all, we can use the computation of Section 3.2 of the entanglement asymmetry (3.27) of a CFT_d in the Rindler geometry to determine the asymmetry of a thermal state in hyperbolic space. We already introduced flat coordinates $\{z_1, z_2, y_{i=1, \dots, d-2}\}$ on \mathbb{R}^d , where z_1 is Euclidean time, so that the subsystem A is the half-space $A = \{z_1 = 0, z_2 \geq 0\}$. We also introduced a complex coordinate

$$z = z_2 + iz_1 = r e^{i\tau} \quad (4.1)$$

so that the metric takes the form $ds_{\text{Rindler}}^2 = dr^2 + r^2 d\tau^2 + dy_{1, \dots, d-2}^2$ with $\tau \cong \tau + 2\pi$. Without loss of generality, we took the insertions at z_{\pm} with $y_i = 0$, as in (3.20). We now perform a conformal (Weyl) transformation to $S^1 \times \mathbb{H}^{d-1}$:

$$ds_{\text{hyper}}^2 = d\tau^2 + \frac{dr^2 + dy_{1, \dots, d-2}^2}{r^2} = \frac{1}{r^2} ds_{\text{Rindler}}^2. \quad (4.2)$$

This maps the subsystem A of the Rindler geometry to the whole hyperbolic space \mathbb{H}^{d-1} at $\tau = 0$. Since entanglement asymmetry transforms as a two-point function, it follows that $\Delta S_{\text{hyper}}^{(2)} = r^{2\Delta} \Delta S_{\text{Rindler}}^{(2)}$ and therefore

$$\Delta S_{\text{hyper}}^{(2)} = I_{\Delta} \left(\tan\left(\frac{\tau_0}{2}\right) \right) \quad (4.3)$$

where $\tau_0 = \frac{1}{2}(\tau_- + \tau_+)$ and I_{Δ} is as in (3.26). This is the entanglement asymmetry of an excited thermal state (with inverse temperature $\beta = 2\pi$) on the hyperbolic plane. It only depends on τ_0 (related to the Euclidean time of the insertions with respect to the cut) and not on the location on the hyperbolic plane because of its $SO(d-1, 1)$ isometry.

¹¹This is the same as what was done in [34, 35, 37] for the entanglement entropy.

¹²In $d = 2$ dimensions, the hyperbolic plane at finite temperature is identical to the standard real line at finite temperature.

It is convenient to rewrite the metric on the hyperbolic geometry as

$$ds_{\text{hyper}}^2 = d\tau^2 + du^2 + \sinh^2(u) d\Omega_{d-2}^2 = \frac{dz d\bar{z}}{|z|^2} + \frac{1}{4} \left| z - \frac{1}{z^*} \right|^2 d\Omega_{d-2}^2 \quad (4.4)$$

where $z = e^{u+i\tau}$ is some other complex coordinate,¹³ while $d\Omega_{d-2}^2$ is the angular metric on a unit sphere S^{d-2} . Notice that in $d > 2$ we take $u \geq 0$ and so $|z| \geq 1$, while in $d = 2$ we can neglect $d\Omega_{d-2}^2$ but take $u \in \mathbb{R}$. We consider a conformal (holomorphic) transformation

$$z = f(w) \quad \text{where} \quad w = r + it_{\text{E}} \quad (4.5)$$

and t_{E} is Euclidean time. The metric takes the form

$$ds_{\text{hyper}}^2 = \left| \frac{f'(w)}{f(w)} \right|^2 \left[dw d\bar{w} + \frac{(|f|^2 - 1)^2}{4|f'|^2} d\Omega_{d-2}^2 \right] \equiv \Omega^2 ds_{\text{geom}}^2. \quad (4.6)$$

This allows us to obtain the asymmetry in other geometries. We will be interested in transformations such that the coefficient of $d\Omega_{d-2}^2$ is only a function of r and not of t_{E} . In any case, the conformal factor Ω and the parameter x are given by

$$\Omega = \left| \frac{f'(w_-)}{f(w_-)} \right|, \quad x \equiv \tan\left(\frac{\tau_0}{2}\right) = -i \frac{z_- + |z_-|}{z_- - |z_-|} = -i \frac{f(w_-) + |f(w_-)|}{f(w_-) - |f(w_-)|}. \quad (4.7)$$

We thus obtain the general formula

$$\Delta S_{\text{geom}}^{(2)} = \Omega^{2\Delta} I_{\Delta}(x). \quad (4.8)$$

4.1 Asymmetry for a finite subregion

The choice

$$z = f(w) = \frac{w + \ell}{\ell - w} \quad (4.9)$$

in (4.6) gives the flat metric $ds_{\text{geom}}^2 = dt_{\text{E}}^2 + dr^2 + r^2 d\Omega_{d-2}^2$ on \mathbb{R}^d . In $d > 2$ dimensions, the preimage of the hyperbolic plane is the spherical region $A = \{t_{\text{E}} = 0, r^2 \leq \ell^2\}$ of radius ℓ that we will call a disk. In $d = 2$ it is convenient to take $r \in \mathbb{R}$ and then the subsystem A is the finite interval $r \in [-\ell, \ell]$. Using (4.7)–(4.8) we can thus compute the entanglement asymmetry of a finite spherical subregion. The conformal factor and the variable x in this case read:

$$\Omega = \frac{2\ell}{|w_-^2 - \ell^2|}, \quad x = \frac{2\ell \Im(w_-)}{\ell^2 - |w_-|^2 - |w_-^2 - \ell^2|}, \quad (4.10)$$

in terms of the insertion point w_- , and $\Delta S_{\text{disk}}^{(2)} = \Omega^{2\Delta} I_{\Delta}(x)$ according to (4.8).

¹³The coordinate change from (4.2) to (4.4) is $(1 + r^2 + \vec{y}^2)/2r = \cosh(u)$, $(1 - r^2 - \vec{y}^2)/2r = \sinh(u) \theta_{d-1}$, $y^j/r = \sinh(u) \theta_j$ for $j = 1, \dots, d-2$, so that $\theta_{a=1, \dots, d-1} \in S^{d-2}$ satisfy $\sum_a \theta_a^2 = 1$.

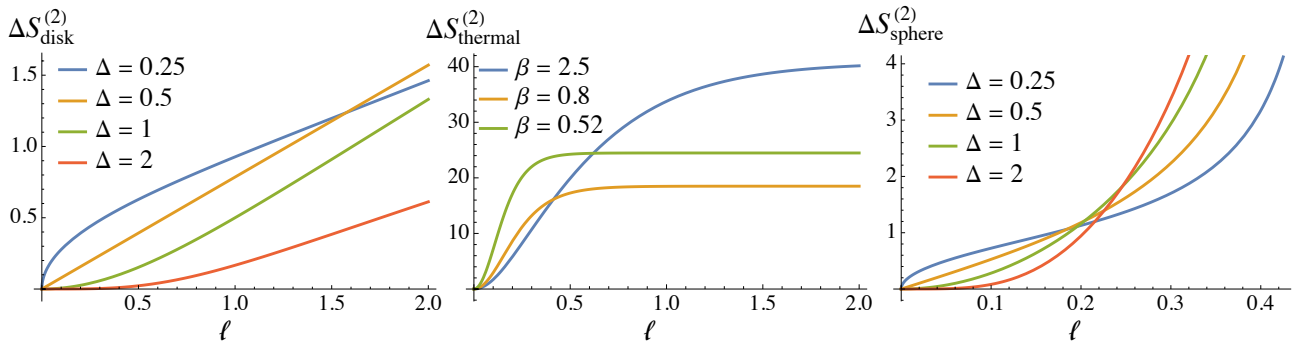


Figure 4: Entanglement asymmetries in various geometries for insertions along the imaginary lines. Left: asymmetry $\Delta S_{\text{disk}}^{(2)}$ of a finite subregion as function of ℓ , for $\eta = 1$. Center: asymmetry $\Delta S_{\text{thermal}}^{(2)}$ at finite temperature β^{-1} as function of ℓ , for $\Delta = 1$ and $\eta = \frac{1}{4}$. Right: asymmetry $\Delta S_{\text{sphere}}^{(2)}$ in finite volume as function of ℓ , for $L = 1$ and $\eta = \frac{1}{3}$ (central line).

These formulas simplify if we take the insertion point w_- to lie along the imaginary axis $\Re(w) = 0$. This is a vertical line (along Euclidean time) that goes through the center of the disk. Let us set¹⁴

$$w_- = -i\eta \quad (4.11)$$

in terms of a real parameter $\eta \in \mathbb{R}_+$. Then

$$\Omega = \frac{2\ell}{\ell^2 + \eta^2} \quad \text{and} \quad x = \tan\left(\frac{\tau_0}{2}\right) = \frac{\ell}{\eta}. \quad (4.12)$$

We thus obtain the following compact expression for the entanglement asymmetry of a disk in infinite volume:

$$\Delta S_{\text{disk}}^{(2)} = \left(\frac{2\ell}{\ell^2 + \eta^2}\right)^{2\Delta} I_{\Delta}\left(\frac{\ell}{\eta}\right). \quad (4.13)$$

In Appendix C we perform a check of this result by computing it in 2d from a four-point function of V , V^\dagger and two twist operators (as in [34]), instead of using geometric replicas. In Fig. 4 (left) we plot the behavior of $\Delta S_{\text{disk}}^{(2)}$ with ℓ for some values of the parameters. The expression in (4.13) has the following asymptotic behaviors:

$$\ell \ll \eta : \quad \Delta S_{\text{disk}}^{(2)} \simeq \frac{\sqrt{\pi} \Gamma(\Delta + 1)}{2 \Gamma(\Delta + \frac{3}{2})} \frac{\ell^{2\Delta}}{\eta^{4\Delta}}, \quad \eta \ll \ell : \quad \Delta S_{\text{disk}}^{(2)} \simeq \frac{\pi \Delta}{4\Delta} \frac{\ell}{\eta^{2\Delta+1}}. \quad (4.14)$$

In particular $\Delta S^{(2)}$ increases and diverges as ℓ for large intervals. We believe that this behavior will be corrected asymptotically by higher-order contributions to ΔS . Notice also that $\Delta S^{(2)}$ is dimensionful, in accord with the fact that $\Delta S = \lambda^2 \Delta S^{(2)} + O(\lambda^4)$ and λ has dimensions of length^Δ . A natural normalization (that we will use later on) would be to fix λ in units of η^Δ .

¹⁴This corresponds to $e^{i\tau_0} = (i\eta - \ell)/(i\eta + \ell)$.

4.2 Asymmetry at finite temperature and in finite volume

The choice

$$z = f(w) = \frac{\sinh(\pi(w + \ell)/\beta)}{\sinh(\pi(\ell - w)/\beta)}, \quad (4.15)$$

which implies the identification $w \cong w + i\beta$, when plugged in (4.6) gives

$$ds_{\text{geom}}^2 = dt_{\text{E}}^2 + dr^2 + \frac{\beta^2}{4\pi^2} \sinh^2\left(\frac{2\pi r}{\beta}\right) d\Omega_{d-2}^2. \quad (4.16)$$

This is the metric on $S_\beta^1 \times \mathbb{H}^{d-1}$, where the Euclidean time circle has radius β . In $d > 2$ dimensions we take $r \geq 0$ and the preimage of the hyperbolic plane is the spherical region $A = \{t_{\text{E}} = 0, r^2 \leq \ell^2\}$ inside \mathbb{H}^{d-1} . This geometry therefore describes an excited thermal state (with temperature β^{-1}) on the hyperbolic plane \mathbb{H}^{d-1} (with curvature proportional to β^{-2}), reduced to a spherical subsystem A . Since the state lives on the hyperbolic plane, it does not originate from the standard thermal vacuum. On the other hand, in $d = 2$ dimensions we take $r \in \mathbb{R}$ and the geometry is just $S_\beta^1 \times \mathbb{R}$ while the subsystem A is the interval $r \in [-\ell, \ell]$: this is a finite subsystem in the standard thermal setup. The entanglement asymmetry is given by (4.7)–(4.8).

For insertions along the imaginary axis $w_- = -i\eta$ (we take $0 < \eta < \beta/2$) namely along the Euclidean circle that goes through the center of the disk A , we find

$$\Delta S_{\text{thermal}}^{(2)} = \left(\frac{2\pi\beta^{-1} \sinh(2\pi\ell/\beta)}{\cosh(2\pi\ell/\beta) - \cos(2\pi\eta/\beta)} \right)^{2\Delta} I_\Delta \left(\frac{\tanh(\pi\ell/\beta)}{\tan(\pi\eta/\beta)} \right). \quad (4.17)$$

We plot it in Fig. 4 (center) for some values of the parameters. In the limit $\beta \gg \ell, \eta$ we recover the case (4.13) of a disk in infinite volume. For $\ell \gg \beta$ we have $\tau_0 \simeq \pi(1 - 2\eta/\beta)$ and therefore the asymmetry asymptotes to a constant:

$$\Delta S_{\text{thermal}}^{(2)} \simeq (2\pi/\beta)^{2\Delta} I_\Delta(\cot(\pi\eta/\beta)) \quad \text{for } \ell \gg \beta. \quad (4.18)$$

This reproduces (4.3) for $\beta = 2\pi$.

The choice

$$z = f(w) = \frac{\sin(\pi(w + \ell)/L)}{\sin(\pi(\ell - w)/L)} \quad (4.19)$$

with $0 < \ell < L/2$ in (4.6) gives

$$ds_{\text{geom}}^2 = dt_{\text{E}}^2 + dr^2 + \frac{L^2}{4\pi^2} \sin^2\left(\frac{2\pi r}{L}\right) d\Omega_{d-2}^2. \quad (4.20)$$

This is the metric on $\mathbb{R} \times S^{d-1}$ where the sphere has circumference L . Notice that (4.19) implies the identification $w \cong w + L$. In $d > 2$ dimensions we take $0 \leq r \leq \frac{L}{2}$ and the preimage of the hyperbolic plane is the spherical region $A = \{t_{\text{E}} = 0, r^2 \leq \ell^2\}$ inside the sphere S^{d-1} . In $d = 2$

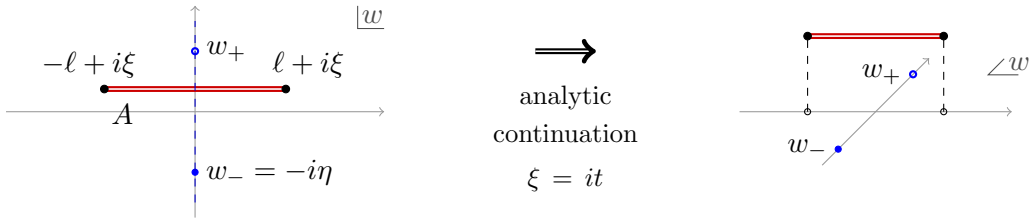


Figure 5: The time evolution of entanglement asymmetry can be computed by first shifting the cut A along the Euclidean time direction by ξ , and then performing analytic continuation $\xi = it$ to Lorentzian time t .

we take $r \cong r + L$ and A is the interval $r \in [-\ell, \ell]$ inside this circle. This geometry allows us to evaluate the asymmetry of a spherical disk in finite volume. The general formula is (4.7)–(4.8).

We consider two interesting cases in which the expressions simplify. One is of insertions along the imaginary axis $w_- = -i\eta$ which is the Euclidean time line through the center of the disk. We call this the central line, and we find

$$\Delta S_{\text{sphere}}^{(2)} = \left(\frac{2\pi L^{-1} \sin(2\pi\ell/L)}{\cosh(2\pi\eta/L) - \cos(2\pi\ell/L)} \right)^{2\Delta} I_{\Delta} \left(\frac{\tan(\pi\ell/L)}{\tanh(\pi\eta/L)} \right). \quad (4.21)$$

We plot it in Fig. 4 (right) for some values of the parameters. Notice that $2\pi\ell/L < \tau_0 < \pi$. For $L \gg \ell, \eta$ we recover the asymmetry (4.13) of a disk in infinite volume. For $\ell \rightarrow L/2$ (*i.e.*, if the subspace A is the whole space) the asymmetry $\Delta S^{(2)}$ diverges, however we believe that this is an artefact of the perturbative expansion. On the other hand, for $\eta \rightarrow \infty$ the asymmetry vanishes because the Euclidean time evolution projects the state to the ground state, which is symmetric.

The other case is of insertions along the axis $\Re(w) = \frac{L}{2}$ that we parametrize as $w_- = \frac{L}{2} - i\eta$. This is the Euclidean time line that goes through the antipodal point on the sphere with respect to the center of the disk, and we call it the antipodal line. We find

$$\Omega = \frac{2\pi L^{-1} \sin(2\pi\ell/L)}{\cosh(2\pi\eta/L) + \cos(2\pi\ell/L)}, \quad x = \tan\left(\frac{\tau_0}{2}\right) = \tan(\pi\ell/L) \tanh(\pi\eta/L), \quad (4.22)$$

and $\Delta S_{\text{sphere}}^{(2)} = \Omega^{2\Delta} I_{\Delta}(x)$. In this case $0 < \tau_0 < 2\pi\ell/L$.

4.3 Time dependence and relaxation

As in [37, 38] we can use conformal transformations and analytic continuation to obtain the time evolution of entanglement asymmetry, as follows. One first computes the entanglement asymmetry of a configuration in which the cut A is shifted by ξ along the Euclidean time direction, as in Fig 5. In our setup, this is equivalent to a geometry in which A is left untouched at $t_E = 0$ but the insertions are shifted as $\mathcal{O}(w_- - i\xi)$ and $\mathcal{O}^\dagger(w_-^* - i\xi)$. Since such a configuration

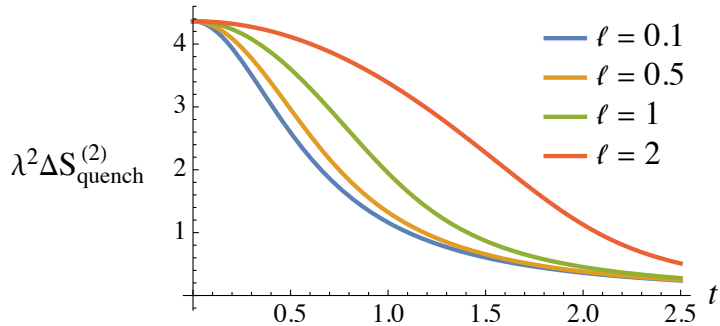


Figure 6: Time evolution of the entanglement asymmetry $\lambda^2 \Delta S_{\text{quench}}^{(2)}(t)$ of a disk after a local quench, for $\eta = 0.6$, $\Delta = 0.5$, and different values of the disk radius ℓ . We normalized $\lambda^2 \propto \ell^{-1}$ in order to have the same initial value. Notice that larger subsystems thermalize more slowly.

is not specular with respect to the spatial slice of the cut at $t_E = 0$, the path integral prepares a “density matrix”

$$\rho_\xi = \text{Tr}_B \left(e^{-(\eta+\xi)H} \mathcal{O} |0\rangle \langle 0| \mathcal{O}^\dagger e^{-(\eta-\xi)H} \right) \quad (4.23)$$

(where $\eta = |\text{Im } w_-|$) which, for real ξ , is not Hermitian. In order to compute the asymmetry of ρ_ξ in general one needs to extend the evaluation of the integral in (3.23) (that computes the asymmetry in the Rindler geometry) to the case that z_\pm have different absolute values. In the thermal hyperbolic geometry, this corresponds to having $\mathcal{O}, \mathcal{O}^\dagger$ inserted at different points on the hyperbolic plane. Then one takes the analytic continuation $\xi = it$, which produces the time-evolved Hermitian density matrix

$$\rho(t) = e^{-itH_A} \rho e^{itH_A}. \quad (4.24)$$

Now the configuration is specular with respect to the spatial slice, the cut is shifted in the Lorentzian time direction, and the path integral is performed along a Schwinger-Keldysh contour. This setup can be regarded as a local quench:¹⁵ at $t = 0$ the system is in an excited state prepared by the Euclidean path integral, and for $t > 0$ it relaxes towards the vacuum.

In the special cases that the orbits of $w_- - i\xi$ and $w_+ - i\xi$ (as we vary ξ) have $|z_-| = |z_+|$ in the Rindler geometry (or equivalently $u_- = u_+$ in the thermal hyperbolic geometry), we can use (3.25). These special cases are precisely the “imaginary lines” we already discussed in the previous sections. Let us discuss the various cases separately.

Finite spherical subregion. We consider the geometry of Section 4.1 with a spherical subsystem $A = \{t_E = 0, r^2 \leq \ell^2\}$ in \mathbb{R}^d and insertions along the imaginary axis $\text{Re}(w) = 0$. With insertions at $w_- = -i(\eta + \xi)$ and $w_+ = i(\eta - \xi)$ we find

$$\tan\left(\frac{\tau_-}{2}\right) = \frac{\ell}{\eta + \xi}, \quad \tan\left(\frac{\tau_+}{2}\right) = \frac{\ell}{\eta - \xi}. \quad (4.25)$$

¹⁵We call the quench “local” (as opposed to “global”) because it is localized in space and it produces an inhomogeneous state.

Including the conformal factors, the entanglement asymmetry takes the form:

$$\Delta S^{(2)} = \left[\frac{4\ell^2}{(\ell^2 + (\eta + \tau)^2)(\ell^2 + (\eta - \tau)^2)} \right]^\Delta I_\Delta \left(\tan^2 \left(\frac{\tau_0}{2} \right) \right) \quad (4.26)$$

where $\tau_0 = \frac{1}{2}(\tau_- + \tau_+)$. We then perform the analytic continuation $\xi = it$ and obtain

$$\Delta S_{\text{quench}}^{(2)} = \left| \frac{2\ell}{\ell^2 + (\eta + it)^2} \right|^{2\Delta} I_\Delta(x) \quad (4.27)$$

where

$$x = \tan \left[\mathbb{R}e \arctan \left(\frac{\ell}{\eta + it} \right) \right] = \frac{\ell^2 - \eta^2 - t^2 + \sqrt{(\ell^2 - \eta^2 - t^2)^2 + 4\ell^2\eta^2}}{2\ell\eta}. \quad (4.28)$$

Both the conformal factor Ω and x are as in (4.10) but evaluated at $w_- = t - i\eta$. This describes the time evolution of entanglement asymmetry after a local quench. We plot $\lambda^2 \Delta S_{\text{quench}}^{(2)}(t)$ for a choice of Δ, η and different values of ℓ in Fig. 6. Using a normalization of λ^2 so as to have the same initial value for the asymmetry, we see that larger subsystems thermalize more slowly. We will explore other physical consequences of (4.27) in Section 4.4.

Finite temperature. For the finite-temperature geometry $S_\beta^1 \times \mathbb{H}^{d-1}$ of Section 4.2 and insertions along the imaginary axis, proceeding as before we find

$$\Delta S_{\text{T quench}}^{(2)} = \left| \frac{2\pi\beta^{-1} \sinh(2\pi\ell/\beta)}{\cosh(2\pi\ell/\beta) - \cos(2\pi(\eta + it)/\beta)} \right|^{2\Delta} I_\Delta(x) \quad (4.29)$$

with

$$x = \tan \left[\mathbb{R}e \arctan \left(\frac{\tanh(\pi\ell/\beta)}{\tan(\pi(\eta + it)/\beta)} \right) \right]. \quad (4.30)$$

The parameter x can also be expressed as in (4.7) with $w_- = t - i\eta$.

Finite volume. For the geometry $\mathbb{R} \times S^{d-1}$ of Section 4.2 and insertions along the imaginary axis (that we called the central line), we find

$$\Delta S_{\text{L quench}}^{(2)} = \left| \frac{2\pi L^{-1} \sin(2\pi\ell/L)}{\cosh(2\pi(\eta + it)/L) - \cos(2\pi\ell/L)} \right|^{2\Delta} I_\Delta(x) \quad (4.31)$$

with

$$x = \tan \left[\mathbb{R}e \arctan \left(\frac{\tan(\pi\ell/L)}{\tanh(\pi(\eta + it)/L)} \right) \right]. \quad (4.32)$$

One can obtain a similar expression for insertions along the antipodal line. In both cases the parameter x can also be expressed as in (4.7) with $w_- = t - i\eta$.

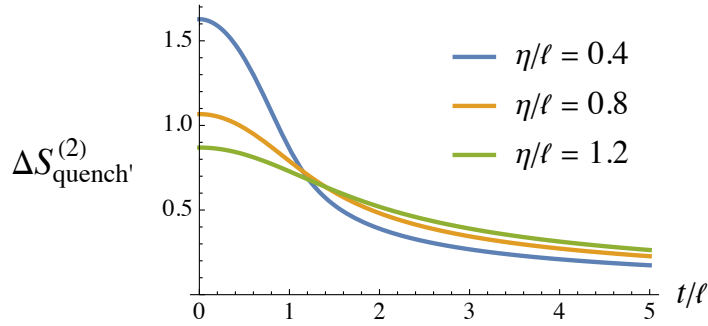


Figure 7: Thermalization curves $\Delta S_{\text{quench}}^{(2)}(t) \equiv \eta^{2\Delta} \Delta S_{\text{quench}}^{(2)}(t)$ for states created with different values of η at fixed $\Delta = 0.2$. We observe the Mpemba effect between any two such curves.

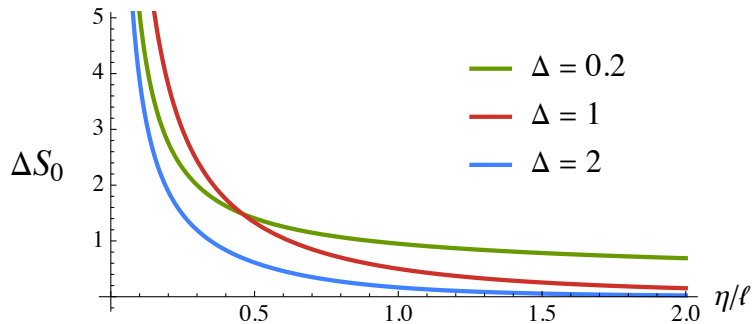


Figure 8: The initial value $\Delta S_0(\eta) = \eta^{2\Delta} \Delta S_{\text{disk}}^{(2)}$ is a decreasing function of η for any fixed Δ . Since the thermalization timescale t_* is an increasing function of η , we always observe the Mpemba effect among states of different η and same Δ , as illustrated in Fig. 7.

4.4 Mpemba effect

In this section we analyze some physical consequences of the time evolution of entanglement asymmetry. Before doing that, notice that the primary operator V has dimensions of mass^Δ while λ has dimensions of length^Δ . It is then more natural to parametrize

$$\lambda = \epsilon \eta^\Delta \tag{4.33}$$

in terms of a (small) dimensionless parameter ϵ . This is the normalization we will use in the rest of this section, hence the entanglement asymmetry takes the form

$$\Delta S = \epsilon^2 \eta^{2\Delta} \Omega^{2\Delta} I_\Delta(x) + O(\epsilon^4) \tag{4.34}$$

at leading order in ϵ .

Let us first study the case of a finite subsystem in infinite volume given by (4.27). Since the conformal factor and the parameter x behave as $\Omega \sim 2\ell/t^2$ and $x \sim \eta\ell/t^2$ for large t , at late times the asymmetry is controlled by the constant $I_\Delta(0)$ and more precisely

$$\Delta S \sim \epsilon^2 \frac{\sqrt{\pi} \Gamma(\Delta + 1)}{2 \Gamma(\Delta + 3/2)} \left(\frac{\eta\ell}{t^2} \right)^{2\Delta} \quad \text{for } t \rightarrow \infty. \tag{4.35}$$

Defining a thermalization timescale t_* as the time at which ΔS gets reduced by a factor of e , we obtain

$$t_* = \sqrt{\eta \ell} e^{1/4\Delta}. \quad (4.36)$$

We see that thermalization is slower if we increase η while it is faster if we increase the conformal dimension Δ . The two parameters η, Δ label the class of states we consider, and it is interesting to compare the thermalization of different states.

Consider two symmetry-breaking states ρ, ρ' and compare how fast they thermalize. How much these states break the symmetry is quantified by the initial value ΔS_0 of the asymmetry at $t = 0$. The speed at which they thermalize is quantified by the corresponding thermalization timescales t_* and t'_* . The Mpemba effect [10–12] occurs when, despite the symmetry being more broken, the thermalization timescale is shorter. This can be expressed using a quantity

$$m = \frac{\Delta S'_0 - \Delta S_0}{t'_* - t_*}. \quad (4.37)$$

If $m \geq 0$ the state starting at a higher ΔS_0 takes more time to equilibrate and there is no Mpemba effect. If $m < 0$, instead, that state relaxes faster, the curves cross, and the Mpemba effect takes place.

If we consider a one-parameter family of states, m evaluated for infinitesimally closed states is related to the derivative of ΔS_0 with respect to the parameter. The sign of the derivative governs whether the Mpemba effect occurs locally around a given state. The result is that the Mpemba effect occurs only in some regions of parameter space. To illustrate this point we analyze two cases: varying η at fixed Δ , and varying Δ at fixed η . In the first case we always observe the Mpemba effect, while in the second case we only observe it using subsystems with $\ell > \eta$ and for sufficiently small conformal dimensions.

Varying η at fixed Δ . This is illustrated in Fig. 7. We always observe the Mpemba effect because any two curves cross. This can be understood from the fact that the initial value $\Delta S_0(\eta)$ is a decreasing function of η (see Fig. 8) and that the thermalization timescale t_* is an increasing function of η .

Varying Δ at fixed η . As illustrated in Fig. 9, we observe two different behaviors depending on the values of the parameters. The two regimes originate from two different profiles of the initial-value curve $\Delta S_0(\Delta)$ plotted in Fig. 10. If the dimension Δ is above a critical value Δ_* , then the Mpemba effect does not take place. If $\Delta < \Delta_*$ then there is Mpemba effect, but this is only visible in subsystems A with $\ell > \eta$. This is because at least one of the two conformal dimensions must be below the value Δ_* at which ΔS_0 has a maximum: The condition to observe the Mpemba effect is that $\Delta < \Delta'$ with $\Delta S_0(\Delta) < \Delta S_0(\Delta')$ which is possible only if $\Delta < \Delta_*$ and only in the region $\ell > \eta$.

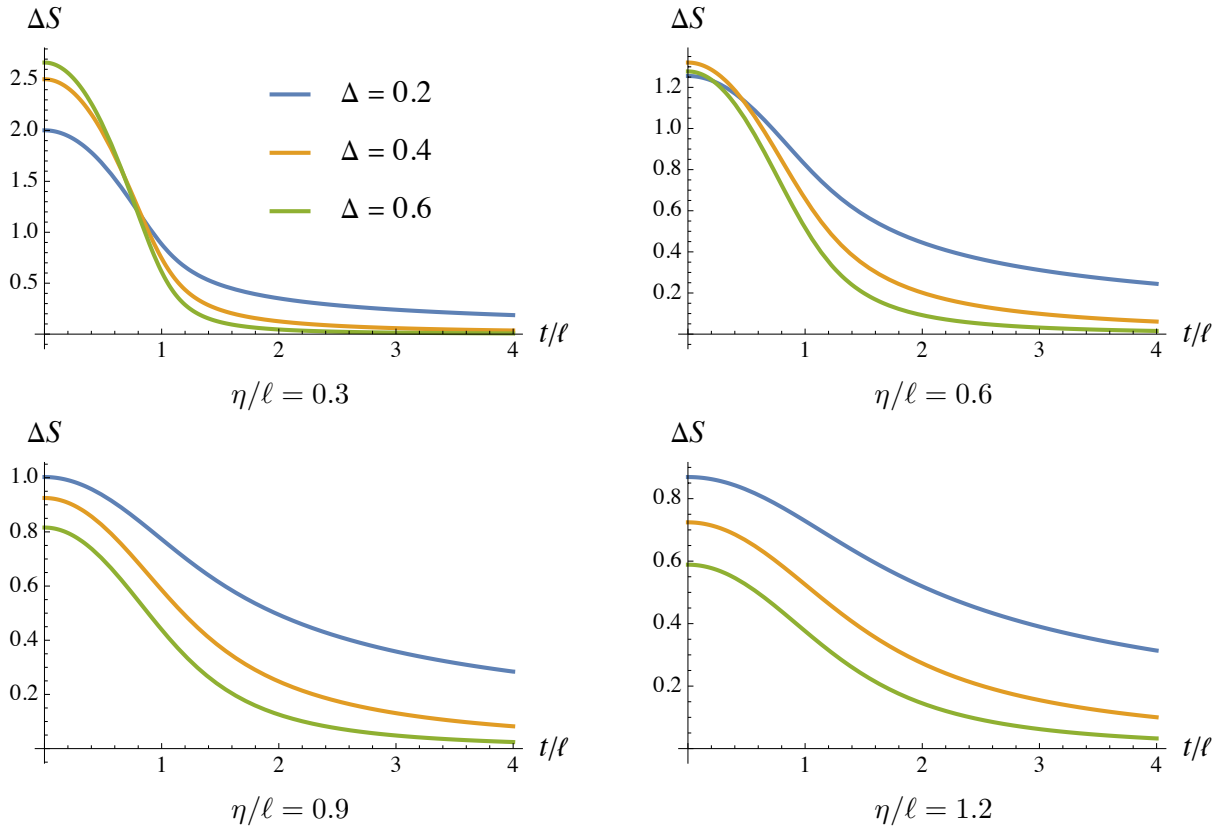


Figure 9: Thermalization for different values of Δ and η . We observe different behaviors in different regions of parameter space. The Mpemba effect is only visible in the two upper plots.

Finite temperature or volume

Next, we can study the finite-temperature case given by $\Delta S_{\text{T quench}}^{(2)}(t)$ in (4.29). At late times the conformal factor behaves as $\Omega \sim 4\pi T \sinh(2\pi T\ell) e^{-2\pi T t}$ where $T = \beta^{-1}$ is the temperature, while $x \rightarrow 0$. This means that at non-vanishing temperature the late-time asymmetry decays exponentially:

$$\Delta S \sim \epsilon^2 \frac{\sqrt{\pi} \Gamma(\Delta + 1)}{2 \Gamma(\Delta + 3/2)} (2\pi T \eta \sinh(2\pi T\ell))^{2\Delta} e^{-4\pi \Delta T t} \quad \text{for } t \rightarrow \infty. \quad (4.38)$$

The natural thermalization timescale is

$$t_* = \frac{1}{\Delta T}. \quad (4.39)$$

The entanglement asymmetry is approximately constant for small times, and then it decays exponentially as illustrated in Fig. 11. For what regards the Mpemba effect, there are four possible regimes depending on the shape of the curve $\Delta S_0(\Delta)$, distinguished by whether $\lim_{\Delta \rightarrow \infty} \Delta S_0$ vanishes or diverges, and by the sign of $\partial_{\Delta} \Delta S_0|_{\Delta=0}$. The four phases are:

- ΔS_0 is a monotonously decreasing function of Δ : we never see the Mpemba effect.
- ΔS_0 first increases and then it decays with Δ : we observe the Mpemba effect for sufficiently small conformal dimensions.

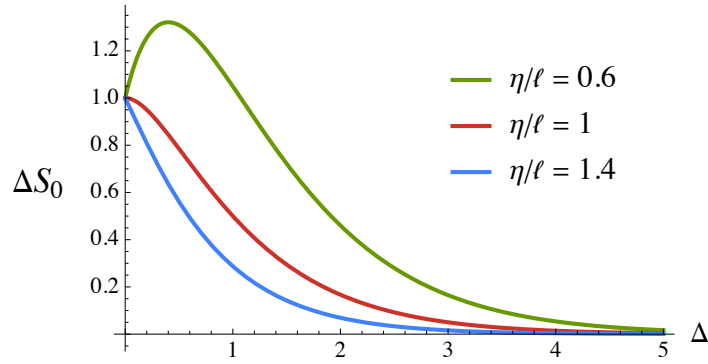


Figure 10: The curve $\Delta S_0(\Delta) = \eta^{2\Delta} \Delta S_{\text{disk}}^{(2)}$ has two different shapes depending on the value of the parameter η . For $\eta \geq \ell$ it is decreasing, while for $\eta < \ell$ it first increases and then decreases.

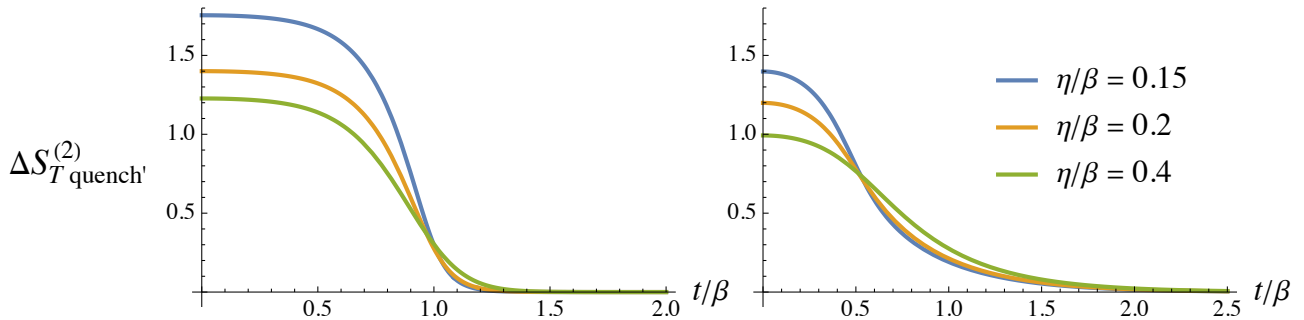


Figure 11: Relaxation of entanglement asymmetry $\Delta S_{T \text{ quench}}^{(2)}(t) = \eta^{2\Delta} \Delta S_{T \text{ quench}}^{(2)}(t)$ at finite temperature β^{-1} , for different values of the parameters. Left plot: $\Delta = 1$ and $\ell/\beta = 1$. Right plot: $\Delta = 0.2$ and $\ell/\beta = \frac{1}{2}$.

- ΔS_0 is monotonously increasing with Δ : we always observe the Mpemba effect.
- ΔS_0 is first decreasing and then diverging with Δ : we see the Mpemba effect for sufficiently large conformal dimensions.

Finally, let us briefly study the time evolution of entanglement asymmetry in finite volume. In Fig. 12 we plot the time dependence of $\Delta S_{L \text{ quench}}^{(2)}(t)$ in (4.31) for different values of the parameter η (that controls insertions along the central line) and a choice of Δ . We observe that the asymmetry is periodic with period L (the circumference of the sphere) and thus it never thermalizes. Although oscillations and partial revivals are expected in systems in finite volume (see for instance [45] for a discussion in two-dimensional rational CFTs), we do not expect exact periodicity in a generic CFT. We believe that this is an artefact of the perturbative expansion, that will be corrected by higher-order terms.

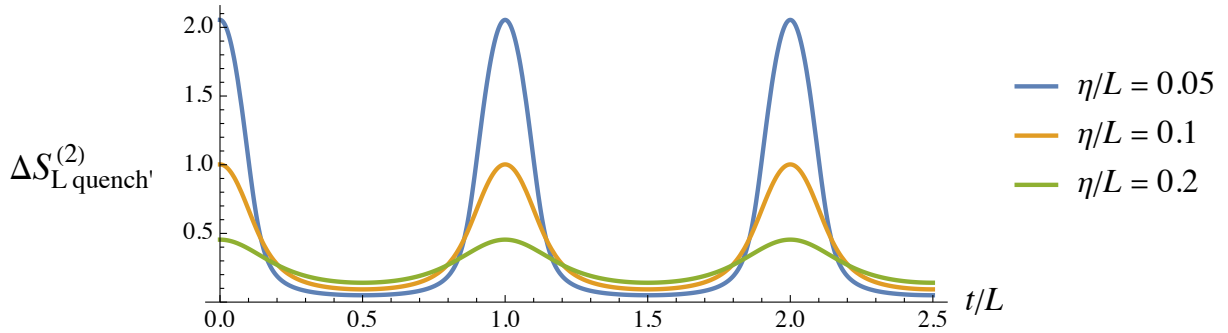


Figure 12: Thermalization in finite volume described by $\Delta S_{L \text{ quench}'}^{(2)}(t) = \eta^{2\Delta} \Delta S_L^{(2)}(t)$ for different values of η . We chose $\Delta = 1$ and subsystem size $\ell = L/8$. We observe a periodic behavior with period L .

5 Asymmetry in holography

The AdS/CFT correspondence [46–48] provides a non-perturbative definition of quantum gravity in AdS space in terms of a CFT that lives at the boundary, such that the bulk direction emerges from the strongly-coupled many-body dynamics of the CFT. Quantum information theory has long been recognized to play a primary role in understanding the emergence of the bulk. The Ryu–Takayanagi formula [49] shows that complicated quantum-information quantities in the CFT can translate to simple geometric observables in AdS, which sometimes can be derived using a gravitational version of the replica trick [50–52]. Thus, it is natural to expect that entanglement asymmetry is also dual to a simple quantity in the bulk. In this section we provide some evidence for this, at leading order in the parameter λ .

5.1 Holographic setup

A holographic CFT $_d$ on \mathbb{R}^d is dual to a bulk gravitational theory in Euclidean AdS $_{d+1}$ with metric (in Poincaré coordinates):

$$ds^2 = \frac{dz^2 + dx_1^2 + \dots + dx_d^2}{z^2}. \quad (5.1)$$

On the boundary we consider states obtained by turning on a source for a charged primary operator V in the Euclidean past:

$$|\psi\rangle = e^{i \int d^d x \lambda(x) V(x)} |0\rangle. \quad (5.2)$$

Such states are of particular interest in holography because they correspond to classical bulk states (see [32] and references therein). When V is charged under a $U(1)$ symmetry, the state $|\psi\rangle$ has nontrivial entanglement asymmetry.

The charged primary V of conformal dimension Δ is dual to a complex scalar field ϕ in the bulk, and its source $\lambda(x)$ corresponds to a boundary condition

$$\lim_{z \rightarrow 0} z^{\Delta-d} \phi(z, x) = \lambda(x). \quad (5.3)$$

The matter theory in the bulk has Euclidean action:

$$S = \int dz d^d x \sqrt{g} \left(\frac{1}{4} F_{\mu\nu} F^{\mu\nu} + |D_\mu \phi|^2 + m^2 |\phi|^2 \right), \quad (5.4)$$

where $D_\mu \phi = \nabla_\mu \phi - ie A_\mu \phi$ and the mass is related to the dimension of V via the formula $m^2 = \Delta(\Delta - d)$. The equations of motion are

$$(D_\mu D^\mu - m^2) \phi = 0, \quad \nabla^\nu F_{\mu\nu} = j_\mu \quad \text{with} \quad j_\mu = -i (\phi^\dagger D_\mu \phi - \phi D_\mu \phi^\dagger), \quad (5.5)$$

where j_μ is the bulk current. The solution that satisfies the boundary condition (5.3) can be written as [48, 53]:

$$\phi(z, x) = \int d^d x' K_E(z, x | x') \lambda(x') \quad (5.6)$$

where the bulk-to-boundary propagator is (for $\Delta > d/2$):

$$K_E(z, x | x') = C_\Delta \left(\frac{z}{z^2 + (x - x')^2} \right)^\Delta. \quad (5.7)$$

The value of C_Δ that reproduces (5.3) is $C_\Delta = \Gamma(\Delta)/(\pi^{d/2} \Gamma(\Delta - d/2))$.¹⁶ However, with that value, the resulting two-point function of the dual complex scalar operator V has coefficient $c = 2(2\Delta - d) \Gamma(\Delta)/(\pi^{d/2} \Gamma(\Delta - d/2))$ (see the Appendix of [53]). In the field theory analysis we normalized the operator V so that its two-point function has coefficient 1. In order to have the same normalization in holography, we should rescale the field ϕ by $c^{-1/2}$. This is the same as rescaling K_E , namely, as taking

$$C_\Delta = \sqrt{\frac{\Gamma(\Delta)}{4 \pi^{d/2} \Gamma(\Delta + 1 - \frac{d}{2})}} \quad (5.8)$$

in (5.7). Notice that the unitarity bound guarantees that $\Delta + 1 - \frac{d}{2} > 0$.

We focus on states where the operator is inserted at a single point:

$$\lambda(x) = \lambda \delta^d(x - x_0), \quad (5.9)$$

and we take $\lambda \in \mathbb{R}$. We consider spherical regions A in the CFT, such that the modular hamiltonian is local and related to the boost generators of half-space by a conformal transformation [54]. As explained in Section 4, the reduced density matrix of A can be obtained by

¹⁶For the case $\Delta = \frac{d}{2}$ in which the mass is at the Breitenlohner-Freedman bound, the asymptotic behavior and the normalizations are different [53].

using a different time slicing of \mathbb{R}^d . This corresponds to writing the metric of \mathbb{R}^d as a conformal transformation of $S^1 \times \mathbb{H}^{d-1}$, namely as

$$ds^2 = \Omega^{-2} (d\tau^2 + du^2 + \sinh^2(u) d\Omega_{d-2}^2) \quad (5.10)$$

as we already did in Section 4.1. The conformal factor (4.10) in these coordinates (for $\ell = 1$) is

$$\Omega = \cosh(u) + \cos(\tau). \quad (5.11)$$

The spherical region A is mapped to the whole hyperbolic plane \mathbb{H}^{d-1} at $\tau = 0$. In the bulk this slicing means writing the AdS metric using coordinates adapted to the Rindler wedge:

$$ds^2 = (\rho^2 - 1) d\tau^2 + \frac{d\rho^2}{\rho^2 - 1} + \rho^2 (du^2 + \sinh^2(u) d\Omega_{d-2}^2) \quad (5.12)$$

with $\rho > 1$. In these coordinates the bulk-to-boundary propagator (5.7) in the embedding formalism reads

$$K_E(\rho, \tau, Y \mid \tau', Y') = \frac{C_\Delta}{(-2\rho Y \cdot Y' - 2\sqrt{\rho^2 - 1} \cos(\tau - \tau'))^\Delta}. \quad (5.13)$$

Here $Y = (Y_0, Y_{a=1, \dots, d-1})$ are coordinates on the hyperboloid \mathbb{H}^{d-1} , they solve the constraint $Y \cdot Y \equiv -Y_0^2 + \sum_a Y_a^2 = -1$ and are parametrized as $Y = (\cosh(u), \sinh(u) \theta_a)$ with $\sum_a \theta_a^2 = 1$ so that $\theta_a \in S^{d-2}$ (see Appendix D and App. A of [32] for more details). The Rindler horizon is at $\rho = 1$ and the asymptotic boundary is at $\rho = \infty$. The prescription of [32], as we review below, requires us to construct a real-time solution for the bulk fields. In particular, the bulk solution is constructed by analytically continuing the propagator (5.13) to $\tau \rightarrow it$. It is then useful at this stage to perform the analytic continuation $\tau = it$ to Lorentzian signature in (5.12) as well, where t is the Lorentzian Rindler time. In these coordinates the bulk modular flow in the Rindler wedge is represented by the manifest Killing symmetry

$$\xi = 2\pi \partial_t. \quad (5.14)$$

The prescription of [32] then, given a spherical region in the CFT $_d$ on $S^1 \times \mathbb{H}^{d-1}$ as before and a one-parameter family of excited states $\rho_A = \sigma_A(1 + i \int d^d x \lambda(x) V(x) + \text{h.c.} + \dots)$, requires us to construct bulk solutions consistent with the operator insertions on the boundary. In hyperbolic coordinates, (5.6) reads

$$\phi(\rho, t, Y) = \int d\tau' dY' K_E(\rho, it, Y \mid \tau', Y') \lambda(\tau', Y') \quad (5.15)$$

with K_E as defined in (5.13) but analytically continued to $\tau \rightarrow it$.

Let us construct these solutions explicitly in Lorentzian AdS $_{d+1}$. The boundary CFT has delta-function sources corresponding to the Euclidean insertion of two conjugate operators V

at $\tau' = -(\pi - \tau_0)$ and V^\dagger at $\tau' = (\pi - \tau_0)$. Without loss of generality we take $u' = 0$. The solution takes the form $\phi(\rho, t, u) = \lambda K_E(\rho, it, u \mid \tau_0 - \pi, 0)$ and similarly for ϕ^\dagger :

$$\begin{aligned}\phi &= \frac{\lambda C_\Delta}{(2\rho \cosh(u) + 2\sqrt{\rho^2 - 1} \cos(it - \tau_0))^\Delta}, \\ \phi^\dagger &= \frac{\lambda C_\Delta}{(2\rho \cosh(u) + 2\sqrt{\rho^2 - 1} \cos(it + \tau_0))^\Delta}.\end{aligned}\tag{5.16}$$

Notice that inserting the boundary operators at specular points $\tau' = \mp(\pi - \tau_0)$ automatically ensures that the bulk solutions are complex conjugate to each other.

5.2 Asymmetry as canonical energy

We saw that, at leading order, entanglement asymmetry is equal to perturbative relative entropy. The latter was shown in [32, 36] to be holographically dual to canonical energy, first defined by Hollands and Wald [55] and then generalized in [56, 57]. This defines a metric on the space of perturbations, known as the “quantum Fisher” or Bogoliubov–Kubo–Mori metric. We therefore conclude that the leading-order entanglement asymmetry is given by the canonical energy, where we are interested in the particular case of scalar primary operator insertions on the boundary, and corresponding dual bulk scalar fields. The canonical energy is defined as a particular symplectic flux of on-shell fields, evaluated on a codimension-one surface in the entanglement wedge which is bounded by the Ryu–Takayanagi surface \tilde{A} on one side and by the boundary subsystem A on the other side. Since the symplectic flux is conserved, we are free to choose any such surface and we choose the $t = 0$ spatial slice of the entanglement wedge.¹⁷ We denote such a surface as Σ , whose boundary is $\partial\Sigma = A \cup \tilde{A}$. The bulk formula for the entanglement asymmetry is

$$\Delta S = \int_\Sigma \star \omega(\phi, \mathcal{L}_\xi \phi) + O(\lambda^4),\tag{5.17}$$

where ϕ is taken of order λ . Here ξ is the vector field of bulk modular flow, which in Rindler coordinates is (5.14), while \mathcal{L}_ξ is a Lie derivative. The symplectic current ω is a one-form, quadratic in the on-shell bulk fields (5.16). We also expect corrections suppressed by G_N and e obtained by taking into account the gravitational and gauge fields.

The symplectic current can be derived by writing the variation of the bulk Lagrangian under a field variation [58]:

$$\delta\mathcal{L} = E_\phi \delta\phi + \nabla^\mu \Theta_\mu[\delta\phi],\tag{5.18}$$

where E_ϕ are the equations of motion. The quantity Θ_μ that produces a total derivative is called the pre-symplectic current. The symplectic current is then defined as [58]:

$$\omega_\mu(\delta_1\phi, \delta_2\phi) = \delta_1\Theta_\mu[\delta_2\phi] - \delta_2\Theta_\mu[\delta_1\phi].\tag{5.19}$$

¹⁷The choice made in [32] is instead that Σ is the horizon of the entanglement wedge.

For the bulk action (5.4), and working in the approximation that only the complex scalar field is turned on at leading order, we find:

$$\begin{aligned}\Theta_\mu[\delta\phi] &= (D_\mu\phi)\delta\phi^\dagger + (D_\mu\phi^\dagger)\delta\phi, \\ \omega_\mu(\phi_1, \phi_2) &= (D_\mu\phi_1)\phi_2^\dagger + (D_\mu\phi_1^\dagger)\phi_2 - (D_\mu\phi_2)\phi_1^\dagger - (D_\mu\phi_2^\dagger)\phi_1.\end{aligned}\tag{5.20}$$

The surface Σ is at $t = 0$. This surface has normal vector $n = (\rho^2 - 1)^{-1/2} \partial_t$ and induced spatial metric

$$ds^2\Big|_{t=0} = \frac{d\rho^2}{\rho^2 - 1} + \rho^2 \left(du^2 + \sinh^2(u) d\Omega_{d-2}^2 \right) \equiv h_{ab} dx^a dx^b.\tag{5.21}$$

The holographic result for the entanglement asymmetry is then

$$\Delta S = \int_1^\infty d\rho \int_0^\infty du \int_{S^{d-2}} d\Omega_{d-2} \sqrt{h} n^\mu \omega_\mu(\phi, \mathcal{L}_\xi\phi) + O(\lambda^4).\tag{5.22}$$

Inserting the solutions (5.16), the integrand takes the explicit form¹⁸

$$\begin{aligned}\int d\Omega_{d-2} \sqrt{h} n^\mu \omega_\mu(\phi, \mathcal{L}_\xi\phi)\Big|_{t=0} &= \\ &= \lambda^2 \frac{C_\Delta^2 \text{Vol}_{S^{d-2}} \pi \Delta \rho^{d-1} \sinh^{d-2}(u) \left(1 + 2\Delta \sin^2(\tau_0) + \rho (\rho^2 - 1)^{-\frac{1}{2}} \cos(\tau_0) \cosh(u) \right)}{4^{\Delta-1} \left(\rho \cosh(u) + \sqrt{\rho^2 - 1} \cos(\tau_0) \right)^{2(\Delta+1)}}.\end{aligned}\tag{5.23}$$

Note that the integral in ρ converges if Δ is larger than the unitarity bound. Although the integral is hard to perform analytically, it is easy to evaluate numerically and we verified that it precisely reproduces the CFT answer:

$$\int_1^\infty d\rho \int_0^\infty du \int d\Omega_{d-2} \sqrt{h} n^\mu \omega_\mu(\phi, \mathcal{L}_\xi\phi) = \lambda^2 \Delta S_{\text{hyper}}^{(2)}\tag{5.24}$$

as given explicitly by eqn. (4.3).

5.3 Relation to the bulk charge

In holography a bulk gauge field A_μ is dual to a boundary current operator. However, there also exists a *bulk* current which, for the action in (5.4), takes the form

$$j_\mu = -i \left(\phi^\dagger D_\mu\phi - \phi D_\mu\phi^\dagger \right).\tag{5.25}$$

This is written in Lorentzian signature where Hermitian conjugation acts in the standard way. Notice that the bulk current is a rather mysterious quantity from the point of view of the boundary CFT. A natural observable is the bulk charge of the Rindler wedge:

$$Q_{\text{bulk}} = \int_\Sigma \star j.\tag{5.26}$$

¹⁸Recall that $\text{Vol}_{S^{d-2}} = 2\pi^{(d-1)/2} / \Gamma\left(\frac{d-1}{2}\right)$.

In AdS_{d+1} it takes the explicit form $Q_{\text{bulk}} = \int_1^\infty d\rho \int_0^\infty du \int d\Omega_{d-2} \sqrt{h} n^\mu j_\mu$ and the integrand reads

$$\int d\Omega_{d-2} \sqrt{h} n^\mu j_\mu \Big|_{t=0} = -\lambda^2 \frac{C_\Delta^2 \text{Vol}_{S^{d-2}} 2\Delta \rho^{d-1} \sinh^{d-2}(u) \sin(\tau_0)}{4^\Delta \sqrt{\rho^2 - 1} (\rho \cosh(u) + \sqrt{\rho^2 - 1} \cos(\tau_0))^{2\Delta+1}}. \quad (5.27)$$

Using the equation of motion $d \star F = \star j$ we can write the integral as

$$Q_{\text{bulk}} = \int_A \star F - \int_{\tilde{A}} \star F, \quad (5.28)$$

where we used that the boundary of the surface Σ is the union of the boundary subsystem A and the Ryu–Takayanagi surface \tilde{A} . The first term simply computes the expectation value of the $U(1)$ charge Q in the CFT:

$$\int_A \star F = \text{Tr}(\rho Q), \quad (5.29)$$

while the second term is the electric flux through the Ryu–Takayanagi surface.

Now, one might expect a relation between bulk charge and entanglement asymmetry. Indeed we observe that, in our setup, the following simple relation holds:

$$\lambda^2 \Delta S^{(2)} = -2\pi \partial_{\tau_0} Q_{\text{bulk}}. \quad (5.30)$$

This follows from the fact that the integrand satisfies (for any t):

$$\omega_\mu(\phi, \mathcal{L}_\xi \phi) = -2\pi \partial_{\tau_0} j_\mu. \quad (5.31)$$

This can be checked explicitly from the formulas given above. It can also be argued from the fact that ∂_{τ_0} acts as $i\partial_t$ on ϕ while it acts as $-i\partial_t$ on ϕ^\dagger in (5.16), due to the general form of the bulk-to-boundary propagator. Indeed a simple calculation shows that

$$\omega_\mu(\phi, \mathcal{L}_\xi \phi) = \left((\partial_\mu \phi) (2\pi \partial_t \phi^\dagger) - (2\pi \partial_\mu \partial_t \phi) \phi^\dagger \right) + \text{h.c.} = -2\pi \partial_{\tau_0} j_\mu. \quad (5.32)$$

This equation is reminiscent of the general analysis carried out in the context of black hole mechanics and Noether charges associated with the symmetries on the black-hole horizon [59, 60]. It would be interesting to investigate this point more systematically.

Notice that τ_0 parametrizes a one-parameter family of solutions as in (5.16), with delta-function sources. One could generalize this setting to a one-parameter family of smeared complex sources labelled by a parameter α :

$$\lambda_\alpha(\tau, Y) = \lambda_0(\tau - \alpha, Y), \quad \lambda_\alpha^*(\tau, Y) = \lambda_0^*(\tau + \alpha, Y), \quad (5.33)$$

where λ_0 and λ_0^* are some reference sources. The effect of α is to shift the boundary conditions along the modular flow. The bulk solutions are then labelled by α as follows:

$$\phi_\alpha(\rho, t, Y) = \int d\tau' dY' K_E(\rho, it, Y \mid \tau', Y') \lambda_\alpha(\tau', Y'). \quad (5.34)$$

Since $\partial_\tau \lambda_\alpha = -\partial_\alpha \lambda_\alpha$ and K_E has translational invariance, one can trade the derivatives with respect to t , τ' and α using integration by parts:

$$\mathcal{L}_\xi \phi_\alpha = -2\pi i \partial_\alpha \phi_\alpha, \quad \mathcal{L}_\xi \phi_\alpha^\dagger = 2\pi i \partial_\alpha \phi_\alpha^\dagger. \quad (5.35)$$

With this, the holographic answer can be written as

$$\Delta S^{(2)} = -2\pi \partial_\alpha \int_\Sigma \star j_\alpha, \quad (5.36)$$

where both sides are of order λ^2 . In other words, the holographic formula (5.30) for the quadratic entanglement asymmetry can be interpreted as the derivative of the bulk charge of the entanglement wedge, with respect to a modular flow of the sources that create the state. It would be interesting to better understand the physical meaning of this observation.

Acknowledgments

We are grateful to Filiberto Ares, Pasquale Calabrese, Laurent Freidel, Giovanni Galati, Max Metlitski and Sridip Pal for helpful discussions. We acknowledge support by the ERC-COG grant NP-QFT No. 864583 “Non-perturbative dynamics of quantum fields: from new deconfined phases of matter to quantum black holes”, by the MUR-FARE grant EmGrav No. R20E8NR3HX “The Emergence of Quantum Gravity from Strong Coupling Dynamics”, by the MUR-PRIN2022 grant No. 2022NY2MXY, and by the INFN “Iniziativa Specifica ST&FP”.

A Renyi asymmetries in 2d CFTs

We compute the Renyi asymmetries in (3.11) for a few semi-integer values of Δ . In particular we have to evaluate the sums

$$P_n = \sum_{j \neq k}^n \frac{1}{\left| 2 \sin \left[\frac{\pi}{n} \left(j - k + \frac{\tau_0}{\pi} \right) \right] \right|^{2\Delta}}. \quad (A.1)$$

We use the Mellin transform (3.12) of $1/\sin(\pi x)$.

Case $\Delta = 1/2$. Taking into account that $\tau_0 \in (0, \pi)$ and therefore for $j > k$ the argument of the sine is between 0 and π while for $j < k$ it is between $-\pi$ and 0, we have

$$\begin{aligned} \Delta S_n^{(2)} &= \frac{n^{-1}}{n-1} \frac{1}{r} \int \frac{ds}{2\pi(1+e^s)} \left[\sum_{j>k}^n e^{\frac{s}{n}(j-k+\frac{\tau_0}{\pi})} + \sum_{j<k}^n e^{\frac{s}{n}(j-k+\frac{\tau_0}{\pi}+n)} \right] \\ &= \frac{n^{-1}}{n-1} \frac{1}{r} \int ds \frac{n(e^{s/n} - e^s)}{2\pi(1+e^s)(1-e^{s/n})} e^{\frac{s\tau_0}{n\pi}}. \end{aligned} \quad (A.2)$$

We can now take the limit $\Delta S^{(2)} = \lim_{n \rightarrow 1} \Delta S_n^{(2)}$ yielding

$$\Delta S^{(2)} = \frac{1}{r} \int \frac{ds s e^{s\tau_0/\pi}}{4\pi \sinh(s)} = \frac{1}{r} \frac{\pi}{8 \cos^2(\frac{\tau_0}{2})}. \quad (\text{A.3})$$

Case $\Delta = 1$. We proceed as before, however this time there are two integrations:

$$\begin{aligned} P_n &= \frac{1}{4\pi^2} \int \frac{ds_1 ds_2}{(1+e^{s_1})(1+e^{s_2})} \left[\sum_{j>k}^n e^{(s_1+s_2)(j-k+\frac{\tau_0}{\pi})/n} + \sum_{j<k}^n e^{(s_1+s_2)(j-k+\frac{\tau_0}{\pi}+n)/n} \right] \\ &= \frac{1}{4\pi^2} \int ds_1 ds_2 \frac{n(e^{(s_1+s_2)/n} - e^{s_1+s_2})}{(1+e^{s_1})(1+e^{s_2})(1-e^{(s_1+s_2)/n})} e^{\frac{(s_1+s_2)\tau_0}{n\pi}}. \end{aligned} \quad (\text{A.4})$$

The integral can be computed analytically. First we change variables setting $s_2 = s - s_1$ and perform the integral in s_1 , obtaining

$$P_n = \int ds \frac{ns}{8\pi^2} e^{\frac{s\tau_0}{n\pi}} \left(\frac{1}{\tanh(s/2n)} - \frac{1}{\tanh(s/2)} \right). \quad (\text{A.5})$$

Then we shift the integration contour from \mathbb{R} to $\mathbb{R} + \pi i$ by redefining $s \rightarrow s + \pi i$, as this does not cross any pole of the integrand. We perform indefinite integration in τ_0 to simplify the expression, and finally integrate in s . We obtain

$$P_n = \partial_{\tau_0} \left[\frac{n^2}{4} \left(\frac{1}{\tan(\tau_0/n)} - \frac{n}{\tan(\tau_0)} - i(n-1) \right) \right] = \frac{n^3}{4 \sin^2(\tau_0)} - \frac{n}{4 \sin^2(\tau_0/n)}. \quad (\text{A.6})$$

This yields the Renyi asymmetry

$$\Delta S_n^{(2)} = \frac{1}{4r^2} \frac{n}{n-1} \left(\frac{1}{\sin^2(\tau_0)} - \frac{1}{n^2 \sin^2(\tau_0/n)} \right) \quad (\text{A.7})$$

and the entanglement asymmetry

$$\Delta S^{(2)} = \frac{1}{2r^2 \sin^2(\tau_0)} \left(1 - \frac{\tau_0}{\tan(\tau_0)} \right). \quad (\text{A.8})$$

Case $\Delta = 3/2$. This time the Renyi asymmetry is given by three integrations:

$$\Delta S_n^{(2)} = \frac{n^{-2}}{n-1} \frac{1}{r^3} \int \frac{ds_1 ds_2 ds_3}{8\pi^3 (1+e^{s_1})(1+e^{s_2})(1+e^{s_3})} \frac{(e^{s/n} - e^s)}{(1-e^{s/n})} e^{\frac{s\tau_0}{n\pi}}, \quad (\text{A.9})$$

where $s = s_1 + s_2 + s_3$. Taking the limit $n \rightarrow 1$ we obtain the entanglement asymmetry

$$\Delta S^{(2)} = \frac{1}{8\pi^3 r^3} \int \frac{ds_1 ds_2 ds_3}{(1+e^{s_1})(1+e^{s_2})(1+e^{s_3})} \frac{s e^{s\tau_0/\pi}}{(1-e^{-s})}. \quad (\text{A.10})$$

It is convenient to change variables to s_1, s_2, s . The integral in s_1 can be easily performed:

$$\Delta S^{(2)} = \frac{1}{8\pi^3 r^3} \int ds_2 ds \frac{s(s-s_2) e^{s\tau_0/\pi}}{(1+e^{-s_2})(e^s - e^{s_2})(1-e^{-s})}. \quad (\text{A.11})$$

Then we shift the integration contour $s \rightarrow s + \pi i$. The integral in s_2 gives

$$\Delta S^{(2)} = \frac{e^{i\tau_0}}{8\pi^3 r^3} \int ds \frac{s(s + \pi i)(s + 2\pi i) e^{s\tau_0/\pi}}{2(1 + e^{-s})(1 - e^s)}. \quad (\text{A.12})$$

The final integral gives the entanglement asymmetry

$$\Delta S^{(2)} = \frac{3\pi}{128 r^3 \cos^4(\frac{\tau_0}{2})}. \quad (\text{A.13})$$

Case $\Delta = 2$. The Renyi asymmetry is given by four integrations. After taking the limit $n \rightarrow 1$ and changing variables to $s = s_1 + s_2 + s_3 + s_4$, we obtain the expression

$$\Delta S^{(2)} = \frac{1}{(2\pi r)^4} \int \frac{ds ds_1 ds_2 ds_3 s e^{s_1+s_2+s_3} e^{s\tau_0/\pi}}{(1 + e^{s_1})(1 + e^{s_2})(1 + e^{s_3})(e^{s_1+s_2+s_3} + e^s)(1 - e^{-s})}. \quad (\text{A.14})$$

We perform the integral in s_1 , and then shift the integration contour $s \rightarrow s + \pi i$:

$$\Delta S^{(2)} = \frac{e^{i\tau_0}}{(2\pi r)^4} \int ds ds_2 ds_3 \frac{(s + \pi i)(s_2 + s_3 - s - \pi i) e^{s\tau_0/\pi}}{(1 + e^{-s_2})(1 + e^{-s_3})(e^{s_2+s_3} + e^s)(1 + e^{-s})}. \quad (\text{A.15})$$

We perform the integral in s_2 , and then shift the integration contour back as $s \rightarrow s - \pi i$:

$$\Delta S^{(2)} = \frac{1}{(2\pi r)^4} \int ds ds_3 \frac{s(s - s_3 - \pi i)(s - s_3 + \pi i) e^{s\tau_0/\pi}}{2(1 + e^{-s_3})(e^{s_3} + e^s)(1 - e^{-s})}. \quad (\text{A.16})$$

We perform the integral in s_3 :

$$\Delta S^{(2)} = \frac{1}{(2\pi r)^4} \int ds \frac{s^2(s^2 + 4\pi^2) e^{s\tau_0/\pi}}{6(e^s - 1)(1 - e^{-s})}. \quad (\text{A.17})$$

The final integration gives the entanglement asymmetry

$$\Delta S^{(2)} = \frac{1}{4r^4 \sin^4(\tau_0)} \left(1 - \frac{1}{3} \sin^2(\tau_0) - \frac{\tau_0}{\tan(\tau_0)} \right). \quad (\text{A.18})$$

B Computation from relative entropy

Let us give some details on the evaluation of the integral (3.25):

$$I_\Delta = - \int_{\mathbb{R}} ds \frac{1}{4 \sinh^2(\frac{s}{2} - i\varepsilon) \left[-4 \sinh^2(\frac{s}{2} - i\tau_0) \right]^\Delta}, \quad (\text{B.1})$$

in terms of the function $I_\Delta(x)$ in (3.26) with $x = \tan(\tau_0/2)$.

First notice that, calling $f(s)$ the integrand in (B.1), it satisfies $f(-s^*) = f(s)^*$. Since the operation $s \rightarrow -s^*$ maps the part of the contour with $s > 0$ to the part with $s < 0$, this implies that the integral can be written as

$$I_\Delta = \int_0^\infty \mathbb{R}e[f(s)], \quad (\text{B.2})$$

showing that the integral is always real. The integrand has poles at $s = 2i\varepsilon + 2\pi ik$ and $s = 2i\tau_0 + 2\pi ik$ for any $k \in \mathbb{Z}$. We thus shift the contour as $s \rightarrow s + 2i\tau_0 - \pi i$. For $0 < \tau_0 < \frac{\pi}{2}$ the contour is moved downward and it does not cross any pole of $f(s)$. On the contrary, for $\frac{\pi}{2} < \tau_0 < \pi$ the contour is moved upward and it crosses the pole at $s = 2i\varepsilon$ where we pick up a residue. We thus obtain the expression

$$I_\Delta = J_\Delta - \delta_{\frac{\pi}{2} < \tau_0 < \pi} \frac{2\pi \Delta}{4^\Delta \sin^{2\Delta}(\tau_0) \tan(\tau_0)} \quad (\text{B.3})$$

where

$$J_\Delta = \int_0^\infty \operatorname{Re} \left[\frac{2^{-2\Delta-1} ds}{\cosh^2\left(\frac{s}{2} + i\tau_0\right) \cosh^{2\Delta}\left(\frac{s}{2}\right)} \right] = \int_0^\infty \frac{(1 + \cos(2\tau_0) \cosh(s)) ds}{2^\Delta (\cos(2\tau_0) + \cosh(s))^2 (1 + \cosh(s))^\Delta}. \quad (\text{B.4})$$

To compute the integral we perform the change of variable $t = \tanh^2\left(\frac{s}{2}\right)$:

$$J_\Delta = \int_0^1 dt \frac{(1+X)(1-tX)(1-t)^\Delta}{2^{2\Delta+1} \sqrt{t} (1+tX)^2} \quad (\text{B.5})$$

where we defined the parameter $X = \tan^2(\tau_0)$. This can be integrated as a hypergeometric function

$$J_\Delta = \frac{\sqrt{\pi} \Gamma(\Delta+1)}{4^\Delta \Gamma(\Delta+\frac{1}{2})} \left(1 - \frac{\Delta}{\Delta+\frac{1}{2}} {}_2F_1\left[\frac{1}{2}, 1, \Delta+\frac{3}{2}; -X\right] \right). \quad (\text{B.6})$$

The hypergeometric function has a branch cut from 1 to infinity, conventionally taken along the positive real axis. When $0 < \tau_0 < \frac{\pi}{2}$ the argument $-X$ of the hypergeometric function goes from 0 to infinity along the negative real axis. For $\tau_0 = \frac{\pi}{2}$ the argument reaches the branch point at infinity and it moves to the second sheet. When $\frac{\pi}{2} < \tau_0 < \pi$ the argument goes from infinity to zero on the second sheet along the negative real axis. The fact that the argument is on the second sheet is implemented by the second term in (B.3).

In order to obtain an equivalent expression that does not require to move between different sheets, it is useful to use a different parameter $x = \tan\left(\frac{\tau_0}{2}\right)$, related to X by

$$X = \frac{4x^2}{(x^2-1)^2}. \quad (\text{B.7})$$

Then one can use hypergeometric transformation identities (see for example [61]) to rewrite the answer in terms of x , obtaining (3.26). A simple way to implement the transformation is to use the fact that the hypergeometric function $y(z) = {}_2F_1(a, b, c; z)$ satisfies a second-order differential equation:

$$z(1-z)y''(z) + (c - (a+b+1)z)y'(z) - aby(z) = 0. \quad (\text{B.8})$$

This implies that the function $I_\Delta \equiv F(X)$ satisfies the differential equation

$$2X(X+1)F''(X) + (2\Delta+5X+3)F'(X) + F(X) = \frac{\sqrt{\pi} \Gamma(\Delta+1)}{4^\Delta \Gamma(\Delta+\frac{1}{2})}. \quad (\text{B.9})$$

We then use the change of variable (B.7) to write a differential equation for the function $I_\Delta \equiv f(x)$ in terms of the parameter x :

$$\frac{(x^2 - 1)^2}{8} f''(x) - \frac{(x^2 - 1)(1 + 3x^2 + (x^2 - 1)^2 \Delta)}{4x(x^2 + 1)} f'(x) + f(x) = \frac{\sqrt{\pi} \Gamma(\Delta + 1)}{4^\Delta \Gamma(\Delta + \frac{1}{2})}. \quad (\text{B.10})$$

Solving this equation again gives the expression in (3.26).

C Asymmetry from twist operators

As in [34], the Renyi asymmetries can be computed by making use of replicated theories, as opposed to replicated geometries. Given a theory \mathcal{S} , we consider a theory $\mathcal{S}^{(n)}$ made of n decoupled copies of \mathcal{S} . Since $\mathcal{S}^{(n)}$ has a permutation symmetry that exchanges the copies, it also has a codimension-two twist operator \mathcal{T}_n such that when we circle around it we go from one copy to the next, cyclicly. More precisely, \mathcal{T}_n is the (non-topological) boundary of a codimension-one topological symmetry defect such that the fields on the two sides are glued with a cyclic permutation. If theory \mathcal{S} has a $U(1)$ symmetry, the previous symmetry defect can be combined with other symmetry defects that implement independent $U(1)$ actions on each copy of \mathcal{S} in $\mathcal{S}^{(n)}$. This generates a dressed twist operator $\mathcal{T}_{n,\gamma}$ that permutes the copies and besides acts with $e^{i\gamma_j Q_A}$ on the j -th copy. The twist operators relevant for the computation of Renyi asymmetries have $\sum_j \gamma_j = 0 \pmod{2\pi}$. Similarly to (2.13), the Renyi asymmetry is then given by a ratio of correlation functions, one with the insertion of the dressed twist fields, and one with the standard twist fields:

$$\Delta S_n = \frac{1}{1-n} \log \frac{\int d\vec{\gamma} \langle \mathcal{T}_{n,\gamma}[\partial A] \dots \rangle}{\langle \mathcal{T}_n[\partial A] \dots \rangle}. \quad (\text{C.1})$$

The twist fields are placed along the boundaries of the cut A . The dots stand for possible operator insertions used to construct the state.

In two dimensions the symmetry defects are lines and the twist operators are pointlike, therefore (C.1) boils down to the computation of certain correlation functions. In this appendix we use (C.1) to compute the Renyi asymmetry of a 2d free Dirac fermion Ψ with respect to its vector-like $U(1)$ symmetry, in coherent states generated by the primary¹⁹ $V = \psi_L \psi_R$ with $\Delta = 1$, for an interval $A = [-\ell, \ell]$. This computation will reproduce (4.13) for $\Delta = 1$, as well as a conformal transformation of (3.13).

The theory $\mathcal{S}^{(n)}$ is given by n copies Ψ_k ($k = 1, \dots, n$) of the 2d free Dirac fermion. The

¹⁹It can be written as $V = \Psi^\top C \Psi$ where C is the charge conjugation matrix.

twist operator $\mathcal{T}_{n,\gamma}(u)$ implements the boundary condition²⁰

$$\begin{aligned}\Psi_k(u + e^{2\pi i}w) &= e^{i\gamma_k} \Psi_{k+1}(u + w) & \text{for } k = 1, \dots, n-1 \\ \Psi_n(u + e^{2\pi i}w) &= (-1)^{n+1} e^{-i(\gamma_1 + \dots + \gamma_{n-1})} \Psi_1(u + w)\end{aligned}\quad (\text{C.2})$$

around u . The twist operator $\mathcal{T}_{n,\gamma}^\dagger$ implements the opposite boundary condition. Writing $\gamma_k = \alpha_{k+1} - \alpha_k$, the boundary conditions are diagonalized by the fields

$$\tilde{\Psi}_l = \frac{1}{\sqrt{n}} \sum_{k=1}^n \exp\left(-2\pi i \frac{2l-n-1}{2n} k + i\alpha_k\right) \Psi_k \quad (\text{C.3})$$

in the sense that

$$\tilde{\Psi}_l(u + e^{2\pi i}w) = e^{2\pi i m_l} \tilde{\Psi}_l(u + w) \quad \text{with} \quad m_l = \frac{2l-n-1}{2n}. \quad (\text{C.4})$$

Notice that in the diagonalizing basis the twists do not depend on the γ_k 's. We decompose the Dirac fermion $\Psi = \begin{pmatrix} \psi_L \\ \psi_R \end{pmatrix}$ into left- and right-moving parts, and the two fields ψ_L and ψ_R have the same charge under $U(1)$. Then the scalar primary we use to construct the excited coherent states is $V = \psi_L \psi_R$.

In order to construct the twist operators we use bosonization. For each copy $\tilde{\Psi}_l$ we introduce a compact scalar²¹ $\varphi \cong \varphi + 2\pi$ and decompose it into left- and right-moving parts: $\varphi = \varphi_L + \varphi_R$ and $\tilde{\varphi} = \varphi_L - \varphi_R$. An operator $\mathcal{O} = e^{i\epsilon_L \varphi_L} e^{i\epsilon_R \varphi_R}$ has dimensions $(h, \bar{h}) = (\epsilon_L^2/2, \epsilon_R^2/2)$. It follows that the fermions are

$$\tilde{\psi}_L = e^{i\varphi_L}, \quad \tilde{\psi}_L^\dagger = e^{-i\varphi_L}, \quad \tilde{\psi}_R = e^{i\varphi_R}, \quad \tilde{\psi}_R^\dagger = e^{-i\varphi_R}. \quad (\text{C.6})$$

The current that implements the shift symmetry $\varphi \rightarrow \varphi + \text{const}$ is $J_\mu = \frac{1}{2\pi} \partial_\mu \varphi$ and the charge operator is $Q = \int \star J = \frac{1}{2\pi} \int d\tilde{\varphi}$. The twist operator lives at the end of a symmetry defect. Thus the operator that implements a twist by $e^{2\pi i\epsilon}$ along the positive real axis, which lives at the left end of the line $e^{2\pi i\epsilon Q}$, is $e^{i\epsilon\tilde{\varphi}} = e^{i\epsilon\varphi_L} e^{-i\epsilon\varphi_R}$ with dimensions $(h, \bar{h}) = (\frac{\epsilon^2}{2}, \frac{\epsilon^2}{2})$ and $\Delta = \epsilon^2$. To resolve possible ambiguities, we insist that the twist operator is the ground state of the twisted sector. This means that we take $\epsilon \in [-\frac{1}{2}, \frac{1}{2}]$. Let us call σ_l the twist operator in the l -th copy that implements a twist by $e^{2\pi i m_l}$. The full twist operator is

$$\mathcal{T}_{n,\gamma} = \prod_{l=1}^n \sigma_l = \prod_{l=1}^n e^{i m_l \tilde{\varphi}_l} \quad (\text{C.7})$$

²⁰This computation is adapted from Section 2.4 of [62]. The minus signs in the second line are due to the fact that we are dealing with fermions, as in thermal partition functions, as explained in Section 2 of [63].

²¹Take $S = \frac{1}{8\pi} \int d^2\sigma \partial_\mu \varphi \partial^\mu \varphi$ with $\varphi \cong \varphi + 2\pi R$. The operators $\mathcal{O}_{n,w} = e^{in\varphi/R} e^{iwR\tilde{\varphi}/2}$ (where the dual scalar $\tilde{\varphi}$ is defined by $\partial_\mu \tilde{\varphi} = \epsilon_{\mu\nu} \partial^\nu \varphi$) have conformal dimensions and spin

$$h_{n,w} = \frac{1}{2} \left(\frac{n}{R} + \frac{wR}{2} \right)^2, \quad \bar{h}_{n,w} = \frac{1}{2} \left(\frac{n}{R} - \frac{wR}{2} \right)^2, \quad \Delta_{n,w} = \frac{n^2}{R^2} + \frac{w^2 R^2}{4}, \quad s_{n,w} = nw. \quad (\text{C.5})$$

T-duality maps $R \leftrightarrow 2/R$. The case $R = 1$ gives the bosonization of the Dirac fermion. Indeed $\mathcal{O}_{\frac{1}{2},1} = \tilde{\psi}_L$ and $\mathcal{O}_{-\frac{1}{2},-1} = \tilde{\psi}_L^\dagger$ are the left-moving fermion while $\mathcal{O}_{\frac{1}{2},-1} = \tilde{\psi}_R$ and $\mathcal{O}_{-\frac{1}{2},1} = \tilde{\psi}_R^\dagger$ are the right-moving fermion.

and its conformal dimension is

$$\Delta[\mathcal{T}_{n,\gamma}] = \sum_{l=1}^n m_l^2 = \frac{n^2 - 1}{12n}. \quad (\text{C.8})$$

This reproduces the dimension of the twist fields in the case of central charge $c = 1$ [34] and shows that such a dimension does not depend on the parameters γ_k [17].

Let us now compute the Renyi asymmetries of the coherent states created by V , for a finite subset $A = [-\ell, \ell]$ as in Section 4.1. For simplicity we take the insertions along the imaginary axis: $w_- = -i\eta$ and $w_+ = i\eta$. The correlator we need to compute is thus

$$\mathcal{A} = \left\langle \mathcal{T}_{n,\gamma}(-\ell) \mathcal{T}_{n,\gamma}^\dagger(\ell) \left(\prod_{j=1}^n e^{i\lambda V_j(-i\eta)} \right) \left(\prod_{j=1}^n e^{-i\lambda V_j^\dagger(i\eta)} \right) \right\rangle_{\mathcal{S}^{(n)}, \mathbb{C}}. \quad (\text{C.9})$$

Here V_j is the primary in the j -th copy, and we put identical insertions in each copy. In (C.1) there is one such correlator in the numerator integrated over $\vec{\gamma}$, and one such correlator in the denominator with $\vec{\gamma} = 0$. We expand the correlator in λ . At zero-th order we have

$$\mathcal{A}^{(0)} = \langle \mathcal{T}_{n,\gamma}(-\ell) \mathcal{T}_{n,\gamma}^\dagger(\ell) \rangle = \frac{1}{(2\ell)^{2\Delta_{\mathcal{T}}}} \quad (\text{C.10})$$

where $\Delta_{\mathcal{T}} = (n^2 - 1)/12n$. At second order we have

$$\mathcal{A}^{(2)} = \left\langle \mathcal{T}_{n,\gamma} \mathcal{T}_{n,\gamma}^\dagger \sum_{k_1, k_2} \left(V_{k_1} V_{k_2}^\dagger \right) \right\rangle, \quad (\text{C.11})$$

where we left the dependence on positions implicit in order not to clutter. We expand each of the fields in the diagonalizing basis:²² the twist operators are as in (C.7) while

$$\begin{aligned} V_{k_1} &= \frac{1}{n} \sum_{j_1, j_2} \exp\left(\frac{2\pi i}{n} (j_1 + j_2 - n - 1) k_1 - 2i\alpha_{k_1} \right) \tilde{\psi}_{Lj_1} \tilde{\psi}_{Rj_2} \\ V_{k_2}^\dagger &= \frac{1}{n} \sum_{j_3, j_4} \exp\left(-\frac{2\pi i}{n} (j_3 + j_4 - n - 1) k_2 + 2i\alpha_{k_2} \right) \tilde{\psi}_{Lj_3}^\dagger \tilde{\psi}_{Rj_4}^\dagger. \end{aligned} \quad (\text{C.12})$$

When we substitute in the correlator (C.11) we obtain six sums. However if we insert $\tilde{\psi}_{Lj_1}$ then there must also be $\tilde{\psi}_{Lj_1}^\dagger$ or else the correlator vanishes, which means that we restrict to $j_3 = j_1$. Similarly we restrict to $j_4 = j_2$. We thus find

$$\begin{aligned} \mathcal{A}^{(2)} &= \frac{1}{n^2} \sum_{k_1, k_2, j_1, j_2} \exp\left[\frac{2\pi i}{n} (j_1 + j_2 - n - 1) (k_1 - k_2) - 2i(\alpha_{k_1} - \alpha_{k_2}) \right] \times \\ &\times \left\langle \left(\prod_l e^{im_l \tilde{\varphi}_l} e^{-im_l \tilde{\varphi}_l} \right) \tilde{\psi}_{Lj_1} \tilde{\psi}_{Rj_2} \tilde{\psi}_{Lj_1}^\dagger \tilde{\psi}_{Rj_2}^\dagger \right\rangle. \end{aligned} \quad (\text{C.13})$$

²²The inverse to (C.3) is $\Psi_k = \frac{1}{\sqrt{n}} \sum_{l=1}^n \exp\left(2\pi i \frac{2l - n - 1}{2n} k - i\alpha_k \right) \tilde{\Psi}_l$.

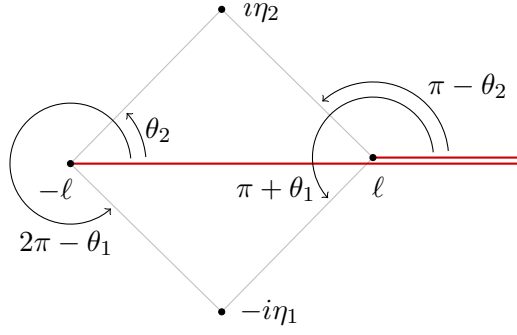


Figure 13: Phases involved in the 4-point function $\langle e^{i\epsilon\varphi_L(-\ell)} e^{-i\epsilon\varphi_L(\ell)} e^{i\varphi_L(-i\eta_1)} e^{-i\varphi_L(i\eta_2)} \rangle$.

In the numerator the integrals over $\vec{\gamma}$, equivalent to integrals over $\vec{\alpha}$, impose $k_1 = k_2$. In the denominator there are no such integrals. So at order λ^2 we are left with a sum over $k_1 \neq k_2$ (and no α 's). We need to compute each term of this sum.

To compute the correlators we use the Coulomb gas formalism, *i.e.*, we separately compute the left- and right-moving contributions. The holomorphic part of a correlator is

$$\langle e^{i\epsilon_1\varphi_L(z_1)} \dots e^{i\epsilon_n\varphi_L(z_n)} \rangle = \prod_{i<j}^n (z_i - z_j)^{\epsilon_i\epsilon_j}. \quad (\text{C.14})$$

The left-moving part of the correlator is given by

$$\begin{aligned} \mathcal{A}_{L,k_1k_2}^{(2)} &= \frac{1}{n} \sum_{j_1=1}^n \left\langle \left(\prod_l e^{im_l\varphi_{Ll}(-\ell)} e^{-im_l\varphi_{Ll}(\ell)} \right) e^{i\varphi_{Lj_1}(-i\eta)} e^{-i\varphi_{Lj_1}(i\eta)} \right\rangle e^{2\pi i \frac{2j_1-n-1}{2n} (k_1-k_2)} \\ &= \left(\prod_{l \neq j_1} (2\ell)^{-m_l^2} \right) \frac{1}{n} \sum_{j_1=1}^n \frac{(2\ell)^{-m_{j_1}^2}}{2i\eta} \left[\frac{(i\eta - \ell)(-i\eta + \ell)}{(i\eta + \ell)(-i\eta - \ell)} \right]^{m_{j_1}} e^{2\pi i \frac{2j_1-n-1}{2n} (k_1-k_2)} \\ &= \frac{n^{-1}}{(2\ell)^{\Delta\tau} (2i\eta)} \sum_{j_1=1}^n e^{2\pi i \frac{2j_1-n-1}{2n} (k_1-k_2 + \frac{\tau_0}{\pi})} = \frac{1}{(2\ell)^{\Delta\tau} (2i\eta)} \frac{\sin(\pi(k_1 - k_2) + \tau_0)}{n \sin(\frac{\pi(k_1-k_2)+\tau_0}{n})}, \end{aligned} \quad (\text{C.15})$$

where $\tau_0 = 2 \arctan(\ell/\eta)$. To correctly evaluate the second line we placed the cut of each twist operator on the right, and this unambiguously fixes all phases. In particular:

$$\begin{aligned} \langle e^{i\epsilon\varphi_L(-\ell)} e^{-i\epsilon\varphi_L(\ell)} e^{i\varphi_L(-i\eta_1)} e^{-i\varphi_L(i\eta_2)} \rangle &= \frac{1}{(2\ell)^{\epsilon^2} i(\eta_1 + \eta_2)} \frac{(i\eta_2 - \ell)^\epsilon (-i\eta_1 + \ell)^\epsilon}{(i\eta_2 + \ell)^\epsilon (-i\eta_1 - \ell)^\epsilon} \\ &= \frac{1}{(2\ell)^{\epsilon^2} i(\eta_1 + \eta_2)} \frac{e^{i(\pi-\theta_2)\epsilon} e^{i(2\pi-\theta_1)\epsilon}}{e^{i\theta_2\epsilon} e^{i(\pi+\theta_1)\epsilon}} = \frac{1}{(2\ell)^{\epsilon^2} i(\eta_1 + \eta_2)} e^{i(2\pi-2\theta_1-2\theta_2)\epsilon}, \end{aligned} \quad (\text{C.16})$$

where $\tan \theta_j = \eta_j/\ell$ and $0 < \theta_j < \frac{\pi}{2}$. Here it is important and all angles are taken from the cut (towards the right) going counterclockwise. See Fig. 13. In our example we take $\theta_1 = \theta_2 \equiv \theta$ and, defining $\tan(\tau_0/2) = \ell/\eta$, we have $\theta = (\pi - \tau_0)/2$. The right-moving part of the correlator is similar, however: $\varphi_{Lj} \rightarrow \varphi_{Rj}$; the twist operator is $e^{-i\epsilon\varphi_R}$; all dependences are on the anti-holomorphic coordinates. This is the same as mapping $\epsilon \rightarrow -\epsilon$ and $\eta \rightarrow -\eta$, and it gives:

$$\mathcal{A}_{R,k_1k_2}^{(2)} = \frac{1}{(2\ell)^{\Delta\tau} (-2i\eta)} \frac{\sin(\pi(k_1 - k_2) + \tau_0)}{n \sin(\frac{\pi(k_1-k_2)+\tau_0}{n})}. \quad (\text{C.17})$$

Putting the two contributions together, we find

$$\mathcal{A}_{k_1 k_2}^{(2)} = \frac{1}{(2\ell)^{2\Delta} 4\eta^2} \frac{\sin^2(\tau_0)}{n^2 \sin^2\left(\frac{\pi(k_1 - k_2) + \tau_0}{n}\right)}. \quad (\text{C.18})$$

The expansion of (C.1) in λ gives

$$\begin{aligned} \Delta S_n &= \frac{1}{1-n} \log \frac{\mathcal{A}^{(0)} + \lambda^2 \frac{1}{(2\pi)^n} \int d\vec{\alpha} \sum_{k_1 k_2} \mathcal{A}_{k_1 k_2}^{(2)}(\vec{\alpha}) + O(\lambda^4)}{\mathcal{A}^{(0)} + \lambda^2 \sum_{k_1 k_2} \mathcal{A}_{k_1 k_2}^{(2)}(0) + O(\lambda^4)} \\ &= \frac{1}{1-n} \log \frac{1 + \frac{\lambda^2}{\mathcal{A}^{(0)}} \sum_k \mathcal{A}_{kk}^{(2)} + O(\lambda^4)}{1 + \frac{\lambda^2}{\mathcal{A}^{(0)}} \sum_{k_1 k_2} \mathcal{A}_{k_1 k_2}^{(2)} + O(\lambda^4)} = \frac{\lambda^2}{n-1} \sum_{k_1 \neq k_2}^n \frac{\mathcal{A}_{k_1 k_2}^{(2)}}{\mathcal{A}^{(0)}} + O(\lambda^4). \end{aligned} \quad (\text{C.19})$$

The sum over $k_1 \neq k_2$ is essentially the same one that we already encountered in (A.1) for $\Delta = 1$. Therefore at quadratic order:

$$\Delta S_n^{(2)} = \frac{1}{n-1} \frac{1}{4\eta^2} \left(n - \frac{\sin^2(\tau_0)}{n \sin^2(\tau_0/n)} \right). \quad (\text{C.20})$$

This is indeed the Renyi asymmetry of an interval in the case $\Delta = 1$, that one obtains by performing a conformal transformation from the Rindler geometry and using (3.13). The limit $n \rightarrow 1$ gives $\Delta S_{\text{disk}}^{(2)} = (1 - \tau_0 \cot(\tau_0))/2\eta^2$ that reproduces (4.13).

D Embedding formalism

In Poincaré coordinates, the metric of Euclidean AdS_{d+1} is

$$ds^2 = \frac{dz^2 + dx_1^2 + \dots + dx_d^2}{z^2} \quad (\text{D.1})$$

where $z > 0$. This can be obtained from the embedding formalism by introducing constrained coordinates $P_A = (P_{-1}, P_0, \dots, P_d)$ that satisfy

$$P \cdot P \equiv -P_{-1}^2 + P_0^2 + \sum_{i=1}^d P_i^2 = -1, \quad P_{-1} \geq 1, \quad (\text{D.2})$$

and projecting the flat metric $ds^2 = -dP_{-1}^2 + dP_0^2 + \sum_{i=1}^d dP_i^2$. This displays the $SO(d+1, 1)$ isometry. The Poincaré coordinates are obtained from the parametrization

$$P_{-1} = \frac{1 + z^2 + \vec{x}^2}{2z}, \quad P_0 = \frac{1 - z^2 - \vec{x}^2}{2z}, \quad P_{i=1, \dots, d} = \frac{x_i}{z}. \quad (\text{D.3})$$

Here $\vec{x} = (x_i) = (x_1, \dots, x_d)$. The conformal boundary is at $z = 0$.

The Rindler coordinates appearing in (5.12) are obtained from the parametrization

$$P_{-1} = \rho Y_0, \quad P_0 = \sqrt{\rho^2 - 1} \cos(\tau), \quad P_d = \sqrt{\rho^2 - 1} \sin(\tau), \quad P_{a=1, \dots, d-1} = \rho Y_a, \quad (\text{D.4})$$

where $\rho \geq 1$, the variable $\tau \in [0, 2\pi)$ is an angle, while (Y_0, Y_a) are auxiliary coordinates on \mathbb{H}^{d-1} that satisfy $-Y_0^2 + \sum_{a=1}^{d-1} Y_a^2 = -1$ and $Y_0 \geq 1$. We parametrize them as

$$Y_0 = \cosh(u), \quad Y_{a=1, \dots, d-1} = \sinh(u) \theta_a, \quad (\text{D.5})$$

where $u \geq 0$ (although in the case of $d = 2$ we could set $\theta_1 = 1$ and use $u \in \mathbb{R}$) while θ_a satisfy $\sum_{a=1}^{d-1} \theta_a^2 = 1$ and describe a sphere S^{d-2} of radius 1. The induced metric is (5.12):

$$ds^2 = (\rho^2 - 1) d\tau^2 + \frac{d\rho^2}{\rho^2 - 1} + \rho^2 \left(du^2 + \sinh^2(u) d\Omega_{d-2}^2 \right) \quad (\text{D.6})$$

where $d\Omega_{d-2}^2$ is the metric on S^{d-2} induced from $ds^2 = \sum_a d\theta_a^2$. The two parametrizations of P_A given above define the change of coordinates.

In Poincaré coordinates the bulk-to-boundary propagator is as in (5.7):

$$K_E(z, \vec{x} \mid \vec{x}') = C_\Delta \left(\frac{z}{z^2 + (\vec{x} - \vec{x}')^2} \right)^\Delta. \quad (\text{D.7})$$

In order to derive the propagator in Rindler coordinates we use the identity

$$\begin{aligned} -2\rho Y \cdot Y' - 2\sqrt{\rho^2 - 1} \cos(\tau - \tau') &= 2 \left[P_{-1} Y'_0 - P_0 \cos(\tau') - P_a Y'_a - P_d \sin(\tau') \right] \\ &= (Y'_0 + \cos(\tau')) \frac{z^2 + (\vec{x} - \vec{x}')^2}{z} \end{aligned} \quad (\text{D.8})$$

where²³

$$x'_a = \frac{Y'_a}{Y'_0 + \cos(\tau')}, \quad x'_d = \frac{\sin(\tau')}{Y'_0 + \cos(\tau')}, \quad \vec{x}'^2 = \frac{Y'_0 - \cos(\tau')}{Y'_0 + \cos(\tau')}. \quad (\text{D.9})$$

The primed coordinates identify a point on the conformal boundary. In Poincaré coordinates, the metric induced on the conformal boundary at $z = 0$ from (D.1) is the flat one of \mathbb{R}^d , namely $ds_\partial^2 = d\vec{x}'^2$. In these coordinates we regard x'_d as the Euclidean time, and consider the spherical spatial subregion $A = \{x'_d = 0, \vec{x}'^2 < 1\}$ where the second term indicates the Euclidean norm of the spatial coordinates. The change of boundary coordinates (D.9) gives

$$ds_\partial^2 = d\vec{x}'^2 = \Omega^{-2} \left(d\tau'^2 + du'^2 + \sinh^2(u') d\Omega_{d-2}^2 \right), \quad \Omega = \cosh(u') + \cos(\tau'). \quad (\text{D.10})$$

Here Ω is precisely the conformal factor (5.11), also appearing in (D.8). The metric in parenthesis is the one of $S^1 \times \mathbb{H}^{d-1}$, which is also the metric on the conformal boundary at $\rho = \infty$ induced from (D.6). The spherical spatial subregion A is mapped to a copy of \mathbb{H}^{d-1} at $\tau' = 0$. Since the propagator transforms as a primary of dimension Δ , using (D.8) we conclude that

$$K_E(\rho, \tau, Y \mid \tau', Y') = \frac{C_\Delta}{\left(-2\rho Y \cdot Y' - 2\sqrt{\rho^2 - 1} \cos(\tau - \tau') \right)^\Delta}. \quad (\text{D.11})$$

²³To invert these formulas (we omit primes) one can use $x_d = \frac{\sin(\tau)}{Y_0 + \cos(\tau)}$, $\frac{1 - \vec{x}^2}{2} = \frac{\cos(\tau)}{Y_0 + \cos(\tau)}$ from which one extracts $\tan(\tau) = \frac{2x_d}{1 - \vec{x}^2}$ and $Y_0 = \frac{1 + \vec{x}^2}{\sqrt{(1 - \vec{x}^2)^2 + 4x_d^2}} \geq 1$.

References

- [1] A. C. Wall, “A proof of the generalized second law for rapidly changing fields and arbitrary horizon slices,” *Phys. Rev. D* **85** (2012) 104049, [arXiv:1105.3445 \[gr-qc\]](#). [Erratum: *Phys.Rev.D* 87, 069904 (2013)].
- [2] H. Casini and M. Huerta, “On the RG running of the entanglement entropy of a circle,” *Phys. Rev. D* **85** (2012) 125016, [arXiv:1202.5650 \[hep-th\]](#).
- [3] T. Faulkner, R. G. Leigh, O. Parrikar, and H. Wang, “Modular Hamiltonians for Deformed Half-Spaces and the Averaged Null Energy Condition,” *JHEP* **09** (2016) 038, [arXiv:1605.08072 \[hep-th\]](#).
- [4] T. Faulkner, M. Guica, T. Hartman, R. C. Myers, and M. Van Raamsdonk, “Gravitation from Entanglement in Holographic CFTs,” *JHEP* **03** (2014) 051, [arXiv:1312.7856 \[hep-th\]](#).
- [5] A. Almheiri, X. Dong, and D. Harlow, “Bulk Locality and Quantum Error Correction in AdS/CFT,” *JHEP* **04** (2015) 163, [arXiv:1411.7041 \[hep-th\]](#).
- [6] G. Penington, “Entanglement Wedge Reconstruction and the Information Paradox,” *JHEP* **09** (2020) 002, [arXiv:1905.08255 \[hep-th\]](#).
- [7] A. Almheiri, N. Engelhardt, D. Marolf, and H. Maxfield, “The entropy of bulk quantum fields and the entanglement wedge of an evaporating black hole,” *JHEP* **12** (2019) 063, [arXiv:1905.08762 \[hep-th\]](#).
- [8] J. de Boer, V. Godet, J. Kastikainen, and E. Keski-Vakkuri, “Quantum information geometry of driven CFTs,” *JHEP* **09** (2023) 087, [arXiv:2306.00099 \[hep-th\]](#).
- [9] F. Ares, S. Murciano, and P. Calabrese, “Entanglement asymmetry as a probe of symmetry breaking,” *Nature Commun.* **14** (2023) 2036, [arXiv:2207.14693 \[cond-mat.stat-mech\]](#).
- [10] E. B. Mpemba and D. G. Osborne, “Cool?,” *Phys. Educ.* **4** (1969) 172.
- [11] Z. Lu and O. Raz, “Nonequilibrium thermodynamics of the Markovian Mpemba effect and its inverse,” *PNAS* **114** (2017) 5083–5088, [arXiv:1609.05271 \[cond-mat.stat-mech\]](#).
- [12] A. Kumar and J. Bechhoefer, “Exponentially faster cooling in a colloidal system,” *Nature* **584** (2020) 64–68, [arXiv:2008.02373 \[cond-mat.stat-mech\]](#).
- [13] L. K. Joshi *et al.*, “Observing the Quantum Mpemba Effect in Quantum Simulations,” *Phys. Rev. Lett.* **133** (2024) 010402, [arXiv:2401.04270 \[quant-ph\]](#).

- [14] F. Ares, S. Murciano, E. Vernier, and P. Calabrese, “Lack of symmetry restoration after a quantum quench: An entanglement asymmetry study,” *SciPost Phys.* **15** (2023) 089, [arXiv:2302.03330 \[cond-mat.stat-mech\]](#).
- [15] B. Bertini, K. Klobas, M. Collura, P. Calabrese, and C. Rylands, “Dynamics of charge fluctuations from asymmetric initial states,” *Phys. Rev. B* **109** (2024) 184312, [arXiv:2306.12404 \[cond-mat.stat-mech\]](#).
- [16] F. Ferro, F. Ares, and P. Calabrese, “Non-equilibrium entanglement asymmetry for discrete groups: the example of the XY spin chain,” *J. Stat. Mech.* **02** (2024) 023101, [arXiv:2307.06902 \[cond-mat.stat-mech\]](#).
- [17] L. Capizzi and M. Mazzoni, “Entanglement asymmetry in the ordered phase of many-body systems: the Ising field theory,” *JHEP* **12** (2023) 144, [arXiv:2307.12127 \[cond-mat.stat-mech\]](#).
- [18] L. Capizzi and V. Vitale, “A universal formula for the entanglement asymmetry of matrix product states,” [arXiv:2310.01962 \[quant-ph\]](#).
- [19] C. Rylands, K. Klobas, F. Ares, P. Calabrese, S. Murciano, and B. Bertini, “Microscopic Origin of the Quantum Mpemba Effect in Integrable Systems,” *Phys. Rev. Lett.* **133** (2024) 010401, [arXiv:2310.04419 \[cond-mat.stat-mech\]](#).
- [20] S. Murciano, F. Ares, I. Klich, and P. Calabrese, “Entanglement asymmetry and quantum Mpemba effect in the XY spin chain,” *J. Stat. Mech.* **01** (2024) 013103, [arXiv:2310.07513 \[cond-mat.stat-mech\]](#).
- [21] M. Chen and H.-H. Chen, “Rényi entanglement asymmetry in (1+1)-dimensional conformal field theories,” *Phys. Rev. D* **109** (2024) 065009, [arXiv:2310.15480 \[hep-th\]](#).
- [22] F. Caceffo, S. Murciano, and V. Alba, “Entangled multiplets, asymmetry, and quantum Mpemba effect in dissipative systems,” *J. Stat. Mech.* **06** (2024) 063103, [arXiv:2402.02918 \[cond-mat.stat-mech\]](#).
- [23] M. Fossati, F. Ares, J. Dubail, and P. Calabrese, “Entanglement asymmetry in CFT and its relation to non-topological defects,” *JHEP* **05** (2024) 059, [arXiv:2402.03446 \[hep-th\]](#).
- [24] S. Yamashika, F. Ares, and P. Calabrese, “Entanglement asymmetry and quantum Mpemba effect in two-dimensional free-fermion systems,” *Phys. Rev. B* **110** (2024) 085126, [arXiv:2403.04486 \[cond-mat.stat-mech\]](#).
- [25] S. Liu, H.-K. Zhang, S. Yin, and S.-X. Zhang, “Symmetry restoration and quantum Mpemba effect in symmetric random circuits,” [arXiv:2403.08459 \[quant-ph\]](#).

- [26] K. Chalas, F. Ares, C. Rylands, and P. Calabrese, “Multiple crossing during dynamical symmetry restoration and implications for the quantum Mpemba effect,” [arXiv:2405.04436 \[cond-mat.stat-mech\]](#).
- [27] F. Ares, V. Vitale, and S. Murciano, “The quantum Mpemba effect in free-fermionic mixed states,” [arXiv:2405.08913 \[cond-mat.stat-mech\]](#).
- [28] X. Turkeshi, P. Calabrese, and A. De Luca, “Quantum Mpemba Effect in Random Circuits,” [arXiv:2405.14514 \[quant-ph\]](#).
- [29] K. Klobas, C. Rylands, and B. Bertini, “Translation symmetry restoration under random unitary dynamics,” [arXiv:2406.04296 \[cond-mat.stat-mech\]](#).
- [30] M. Botta-Cantcheff, P. Martínez, and G. A. Silva, “On excited states in real-time AdS/CFT,” *JHEP* **02** (2016) 171, [arXiv:1512.07850 \[hep-th\]](#).
- [31] A. Christodoulou and K. Skenderis, “Holographic Construction of Excited CFT States,” *JHEP* **04** (2016) 096, [arXiv:1602.02039 \[hep-th\]](#).
- [32] T. Faulkner, F. M. Haehl, E. Hijano, O. Parrikar, C. Rabideau, and M. Van Raamsdonk, “Nonlinear gravity from entanglement in conformal field theories,” *JHEP* **08** (2017) 057, [arXiv:1705.03026 \[hep-th\]](#).
- [33] C. Holzhey, F. Larsen, and F. Wilczek, “Geometric and renormalized entropy in conformal field theory,” *Nucl. Phys. B* **424** (1994) 443–467, [arXiv:hep-th/9403108](#).
- [34] P. Calabrese and J. L. Cardy, “Entanglement entropy and quantum field theory,” *J. Stat. Mech.* **0406** (2004) P06002, [arXiv:hep-th/0405152](#).
- [35] P. Calabrese and J. Cardy, “Entanglement entropy and conformal field theory,” *J. Phys. A* **42** (2009) 504005, [arXiv:0905.4013 \[cond-mat.stat-mech\]](#).
- [36] N. Lashkari and M. Van Raamsdonk, “Canonical Energy is Quantum Fisher Information,” *JHEP* **04** (2016) 153, [arXiv:1508.00897 \[hep-th\]](#).
- [37] J. Cardy and E. Tonni, “Entanglement hamiltonians in two-dimensional conformal field theory,” *J. Stat. Mech.* **1612** (2016) 123103, [arXiv:1608.01283 \[cond-mat.stat-mech\]](#).
- [38] P. Calabrese and J. L. Cardy, “Time-dependence of correlation functions following a quantum quench,” *Phys. Rev. Lett.* **96** (2006) 136801, [arXiv:cond-mat/0601225](#).
- [39] Z. Ma, C. Han, Y. Meir, and E. Sela, “Symmetric inseparability and number entanglement in charge-conserving mixed states,” *Phys. Rev. A* **105** (2022) 042416, [arXiv:2110.09388 \[quant-ph\]](#).
- [40] N. Laflorencie and S. Rachel, “Spin-resolved entanglement spectroscopy of critical spin chains and Luttinger liquids,” *J. Stat. Mech.* **11** (2014) P11013, [arXiv:1407.3779 \[cond-mat.str-el\]](#).

- [41] M. Goldstein and E. Sela, “Symmetry-resolved entanglement in many-body systems,” *Phys. Rev. Lett.* **120** (2018) 200602, [arXiv:1711.09418](#) [`cond-mat.stat-mech`].
- [42] J. C. Xavier, F. C. Alcaraz, and G. Sierra, “Equipartition of the entanglement entropy,” *Phys. Rev. B* **98** (2018) 041106, [arXiv:1804.06357](#) [`cond-mat.stat-mech`].
- [43] D. Gaiotto, A. Kapustin, N. Seiberg, and B. Willett, “Generalized Global Symmetries,” *JHEP* **02** (2015) 172, [arXiv:1412.5148](#) [`hep-th`].
- [44] M. Gutperle, Y.-Y. Li, D. Rathore, and K. Roumpedakis, “A note on entanglement entropy and topological defects in symmetric orbifold CFTs,” *JHEP* **09** (2024) 010, [arXiv:2406.10967](#) [`hep-th`].
- [45] J. Cardy, “Thermalization and Revivals after a Quantum Quench in Conformal Field Theory,” *Phys. Rev. Lett.* **112** (2014) 220401, [arXiv:1403.3040](#) [`cond-mat.stat-mech`].
- [46] J. M. Maldacena, “The Large N limit of superconformal field theories and supergravity,” *Adv. Theor. Math. Phys.* **2** (1998) 231–252, [arXiv:hep-th/9711200](#).
- [47] S. S. Gubser, I. R. Klebanov, and A. M. Polyakov, “Gauge theory correlators from noncritical string theory,” *Phys. Lett. B* **428** (1998) 105–114, [arXiv:hep-th/9802109](#).
- [48] E. Witten, “Anti-de Sitter space and holography,” *Adv. Theor. Math. Phys.* **2** (1998) 253–291, [arXiv:hep-th/9802150](#).
- [49] S. Ryu and T. Takayanagi, “Holographic derivation of entanglement entropy from AdS/CFT,” *Phys. Rev. Lett.* **96** (2006) 181602, [arXiv:hep-th/0603001](#).
- [50] A. Lewkowycz and J. Maldacena, “Generalized gravitational entropy,” *JHEP* **08** (2013) 090, [arXiv:1304.4926](#) [`hep-th`].
- [51] G. Penington, S. H. Shenker, D. Stanford, and Z. Yang, “Replica wormholes and the black hole interior,” *JHEP* **03** (2022) 205, [arXiv:1911.11977](#) [`hep-th`].
- [52] A. Almheiri, T. Hartman, J. Maldacena, E. Shaghoulian, and A. Tajdini, “Replica Wormholes and the Entropy of Hawking Radiation,” *JHEP* **05** (2020) 013, [arXiv:1911.12333](#) [`hep-th`].
- [53] D. Z. Freedman, S. D. Mathur, A. Matusis, and L. Rastelli, “Correlation functions in the CFT_d/AdS_{d+1} correspondence,” *Nucl. Phys. B* **546** (1999) 96–118, [arXiv:hep-th/9804058](#).
- [54] H. Casini, M. Huerta, and R. C. Myers, “Towards a derivation of holographic entanglement entropy,” *JHEP* **05** (2011) 036, [arXiv:1102.0440](#) [`hep-th`].
- [55] S. Hollands and R. M. Wald, “Stability of Black Holes and Black Branes,” *Commun. Math. Phys.* **321** (2013) 629–680, [arXiv:1201.0463](#) [`gr-qc`].

- [56] N. Lashkari, J. Lin, H. Ooguri, B. Stoica, and M. Van Raamsdonk, “Gravitational positive energy theorems from information inequalities,” *PTEP* **12** (2016) 12C109, [arXiv:1605.01075 \[hep-th\]](#).
- [57] A. May and E. Hijano, “The holographic entropy zoo,” *JHEP* **10** (2018) 036, [arXiv:1806.06077 \[hep-th\]](#).
- [58] J. Lee and R. M. Wald, “Local symmetries and constraints,” *J. Math. Phys.* **31** (1990) 725–743.
- [59] R. M. Wald, “Black hole entropy is the Noether charge,” *Phys. Rev. D* **48** (1993) R3427–R3431, [arXiv:gr-qc/9307038](#).
- [60] V. Iyer and R. M. Wald, “Some properties of Noether charge and a proposal for dynamical black hole entropy,” *Phys. Rev. D* **50** (1994) 846–864, [arXiv:gr-qc/9403028](#).
- [61] G. E. Andrews, R. Askey, and R. Roy, *Special functions*. Encyclopedia of mathematics and its applications. Cambridge University Press, 1999.
- [62] A. Belin, L.-Y. Hung, A. Maloney, S. Matsuura, R. C. Myers, and T. Sierens, “Holographic Charged Renyi Entropies,” *JHEP* **12** (2013) 059, [arXiv:1310.4180 \[hep-th\]](#).
- [63] H. Casini, C. D. Fosco, and M. Huerta, “Entanglement and alpha entropies for a massive Dirac field in two dimensions,” *J. Stat. Mech.* **0507** (2005) P07007, [arXiv:cond-mat/0505563](#).